

Point-by-point response to the reviews

Responses to the reviewers are shown in red as Author Comment (AC). The number of the lines where to find the modifications done in the text are those from the Track changes version of the manuscript (see below).

Anonymous Referee #1

The authors test the MAIDENiso model in regard to O-isotope fractionation with “temperature-sensitive” tree species in Quebec and from Patagonia (which I interpret as ring growth being sensitive to temperature). In the case of the Canadian site, the high latitude indicates temperature sensitivity, whereas for the Argentina site the elevation probably contributes more to the temperature sensitivity. A number of parameters in the mechanistic models must be estimated, among which the estimated $\delta^{18}\text{O}$ of precipitation may have the greatest uncertainty, but parameters are also tested for sensitivity in simulating the observed tree-ring $\delta^{18}\text{O}$. The authors found that xylem water $\delta^{18}\text{O}$ is less influential than leaf evaporative enrichment in predicting tree-ring $\delta^{18}\text{O}$. Furthermore, temperature effects are more related to effect on leaf evaporative enrichment than T effects on precipitation isotopes. The analysis is important and results reasonable, although there are some large $\delta^{18}\text{O}$ differences in the actual tree-ring composition between the N. American and S. American sites.

AC: We thanks a lot Reviewer#1 for all his comments and suggestions.

Comments

p. 35, ‘tree rings’

AC: We changed this part as proposed by Reviewer#1 (L30).

p. 101-102, ‘which is an angiosperm deciduous species dominating’

AC: We changed this part as proposed by Reviewer#1 (L103).

p. 111-112, ‘In western Argentina, precipitation is largely concentrated from late fall to early spring followed by a drier and mild period during summer and early fall’: isn’t late fall to early spring summer in Argentina, and therefore the following ‘mild period’ would be during the Argentina winter and early spring?

AC: In western Argentina, precipitation is concentrated in late fall to early spring (May-November) followed by a drier and mild period during summer and early fall (December-April). We specified the respective months for each period in the text (L112-114).

p. 188, ‘for *N. pumilio*, and therefore the’

AC: We changed this part as proposed by Reviewer#1 (L199).

216-217, ‘we also used modelled daily data from the GCMs described above for both the western Argentinian and northeastern Canadian sites’

AC: We changed this part as proposed by Reviewer#1 (L230-231).

221-222, 'For the years 1950-1957,'

AC: We changed this part as proposed by Reviewer#1 (L235).

240 (and 159), the authors refer to 'dampening factor fo', but Eqn1 suggests it is actually the fraction of the tree-ring $\delta^{18}\text{O}$ signal that derives from xylem water: perhaps they are synonymous?

AC: The 'dampening factor' is defined in the literature (e.g. Saurer et al. 1997) as the proportion of oxygen atoms that is exchanged between sucrose and xylem water during cellulose synthesis. It is modelled as a coefficient in Eqn1 to take into account the part of $\delta^{18}\text{O}$ signal derived from xylem water during this exchange that is incorporated in the cellulose $\delta^{18}\text{O}$.

287, in "temperature and precipitation dependences", the authors seem to mean "temperature and precipitation coefficients", i.e., a and b.

AC: Yes, the temperature and precipitation dependences are modelled as coefficients a and b, respectively.

289, "more strongly"

AC: We changed this part as proposed by Reviewer#1 (L307).

319, what is the "reference one"? perhaps "reference simulations"?

AC: Yes, it is the reference simulations. We changed it in the text (L342).

320, what is the "source one"? perhaps "than are the XW_source simulations"?

AC: Idem, we changed it in the text (L343).

325, what does "these results are limited upstream" mean?

AC: We removed this sentence in the text that was not clear (L352).

341-342, change "ratio in a high amount of precipitated water" to "ratio increased higher precipitation"

AC: We have simplified the sentence to be more understandable: 'Consequently, in the Tropics, the $^{18}\text{O}/^{16}\text{O}$ ratio in the meteoric water has been observed to decrease with increasing amount of precipitation and/or relative humidity.' (L365-367).

362-363, why is it 'interesting(ly)' that "the $\delta^{18}\text{O}_p$ signal in northeastern Canada is comparatively more depleted than in western Argentina". Given the latitude of northeastern Canada, I would expect $\delta^{18}\text{O}_p$ to be isotopically lighter.

AC: We expanded a little bit the explanation of why the $\delta^{18}\text{O}_p$ signal in northeastern Canada was comparatively more depleted than in western Argentina, following Reviewer#1 recommendations (L397-399).

363, “northeast”

AC: We decided to keep ‘northeastern’, which is often used (L394).

385-386, “GNIP stations”

AC: We changed this part as proposed by Reviewer#1 (L414).

434-435, “tree growth is inhibited, leading to a decrease of”

AC: We changed this part as proposed by Reviewer#1 (L484).

465, “tree rings”

AC: We changed this part as proposed by Reviewer#1 (L507-508).

719, are the “mean simulated $\delta^{18}\text{O}_{\text{TR}}$ levels” (here in caption and in B y-axis labels) actually “ $\delta^{18}\text{O}_{\text{TR}}$ values”? or “ $\delta^{18}\text{O}_{\text{TR}}$ output”

AC: Yes, they are the simulated $\delta^{18}\text{O}_{\text{TR}}$ values. We decided to stay with ‘simulated $\delta^{18}\text{O}_{\text{TR}}$ levels’ because in this figure we want to show that some parameters are affecting the mean levels of $\delta^{18}\text{O}_{\text{TR}}$ values (L890).

REFERENCES

The “13”s and “18”s in isotope designations in titles need to be superscripted. DeNiro and Epstein 1979, Rozanski et al. 1993, Yakir and Deniro references: too many words in title begin with upper-case letters

AC: We have corrected all the errors detected by Reviewer#1 in the reference list.

Figure 4, shouldn’t the label on the y-axis be “kernel density”?

AC: We think that the y-axis as ‘kernel density estimates’ is fine (L908).

Anonymous Referee #2

This paper is a welcome addition to the literature on tree ring isotopes and their potential to enrich palaeoclimate reconstructions. Application of the MAIDENiso (MI) model to two different species in two different environments was undertaken, and both of the target species have the potential to provide longer palaeoclimate reconstructions. The main aims are made clear from the outset: to evaluate if MI can simulate $\delta^{18}\text{O}$ of tree rings, to identify physical processes that control $\delta^{18}\text{O}$ of tree rings using mechanistic modeling, and assess the origin of how temperature is recorded in both target species.

The mixture of settings and hemispheres is also nice to see. I was also delighted by the fact that this is a well-written paper, and I enjoyed reading it.

AC: We are happy that the reviewer really liked and enjoyed our study.

I have only a few main comments that I believe can help, and a handful of minor ones. For Section 2.4. Estimation of parameters, I believe this is one of the more important elements of the study. It is my opinion here because in some cases, a range of unknowns need to be assumed or tested in a hierarchical way where observations are sparse. It might be good to mention other studies to the readers that have grappled with this issue in this section. For example, a range of unknown parameters for a Southern Hemisphere species with dendroclimatic potential was recently examined using a mechanistic model that augmented Barbour, Roden, Farquhar and Ehleringer (BRFE04). The ranges of some unknown parameters were tested simultaneously against a mean $\delta^{18}\text{O}$ chronology while others were empirically derived (Lorrey et al., 2016). The code for the model described in that paper can be found here: https://github.com/nicolasfauchereau/model_isotope

AC: We have added in the text the link to the code of MAIDENiso model: <https://doi.org/10.6084/m9.figshare.5446435.v1> (L134-135).

I can appreciate that some elements of MI will be different from other mechanistic models that have come before, so my pointing to the aforementioned resource is not to state it is better (or to get it cited), but rather suggesting that a myriad of modelling approaches can be helpful for distilling and probing important issues for isotope dendroclimatology.

AC: We thank Reviewer#2 for this suggestion. We have mentioned in the revised manuscript other studies that have used this approach: e.g. Danis et al., 2012; Lorrey et al., 2016 (see L266-268).

It would also be really nice if a diagram that shows how the MI model was constructed (the main componentry and inputs, for example) could be included either in the main paper or the supplement.

AC: Different publications have already detailed the construction of the MAIDEN model (among the most recent one, Danis et al., 2012 and Gennaretti et al. 2017b). We have cited these papers in the text as references (L126 and L128-129).

Minor comments.

118-120. Rephrase this please as: The chronologies that were built for each species were significantly correlated between stands (Figure 1). This supported the construction of a combined isotope chronology for both the northeastern Canada and western Argentina sites.

AC: We changed this part as proposed by Reviewer#2 (L119-122).

124. please provide reference for MAIDENiso again here. If you can please provide links to the code for this model, it would be appreciated.

AC: We have added the references on MAIDENiso model mentioned above (L126 and L128-129).

162. can you please cite any IAEA studies where the closest measurements would be, or have a look at whether anything useful can be gleaned from the data underpinning the online isotopes in precipitation calculator

AC: To our knowledge, no IAEA studies have been developed in the regions of our study. In Argentina, only studies further north (30°S; Rozanski et al. 1995) and further south (47°-48°S; Stern and Blisniuk, 2002) have been done to understand the variability of $\delta^{18}\text{O}_p$. We are referring to the IAEA dataset in the text (L171-172) and we discussed the studies that have been done further north and further south in the Discussion section (L371-376).

164. First. Not Firstly. Prettification of words by adding 'ly' is not correct grammar.

AC: We have changed it as proposed by Reviewer#2 (L174).

175. As above with secondly. Second.

AC: We have changed it as proposed by Reviewer#2 (L185).

180. can you please spell out the acronym for LMDZ5A, and also fully spell out National Centers for Environmental Protection (NCEP), as well as fully refer to the 20th Century Reanalysis (20CR)

AC: LMDZ5A is the acronym of 'Laboratoire de Météorologie Dynamique Zoom'. We have spelled out all the acronyms in the text as proposed by Reviewer#2 (L190-192).

202. I see 20CRv2c mentioned here; it should be fine, but please explain why this reanalysis dataset is chosen over something like NCEP1 or ERA-Interim.

AC: We have used the 20CRv2c dataset to extract daily minimum-maximum temperatures and precipitation amount because it is one of the few reanalysis products covering entirely the 20th century. Furthermore, NCEP1 has been replaced by 20CRv2c and ERA-Interim starts in 1979. We add this explanation in the text (L218-219).

250. Lorrey et al. (2016) evaluated the outcomes of iterative changes to unknown parameters for a $\delta^{18}\text{O}$ model output in a similar way for NZ kauri (mentioned above). This appears to be a standard way to evaluate how well a mechanistic model does for $\delta^{18}\text{O}_{\text{TR}}$, in a simple way. I would just mention here a range of studies that may have undertaken a similar approach to show it is an acceptable method for evaluation.

AC: As suggested by Reviewer#2, we have added other studies that have undertaken a similar approach (L266-268).

318. Leaf water enrichment (are underscores needed?)

AC: We have deleted the underscores (L280, L287 and L341).

324. Last sentence. Can you please expand on this statement just a little bit more, for clarity?

AC: As suggested as well by Reviewer#1, we have deleted this last sentence, which was not clear (L352).

348. ‘...agreement with previous work (Rozanski et al)’

AC: We changed it as proposed by Reviewer#2 (L373).

356. Reword to start “In contrast, in northeastern Canada...”.

AC: We changed it as proposed by Reviewer#2 (L391).

362. Reword to start “Of interest, the ...”

AC: We changed this sentence as proposed by Reviewer#1 (L397-399).

374. Reword to say “Although isotope-enabled atmospheric global models can reproduce the mean annual precipitation isotopic values and seasonality for many areas (Risi et al)...”

AC: We changed the sentence as proposed by Reviewer#2 (L410-412).

385. Also mention here that the IAEA datasets that had a good deal of chemistry run on them in the 1970-80s may have been compromised by pan evaporation and therefore enrichment. Have to treat many of those extant (older) data sources very carefully.

AC: We have incorporated this explanation as well in the text (L421-436).

471. Firstly. As above.

AC: We changed it as proposed by Reviewer#2 (L521).

473. Secondly. As above.

AC: We changed it as proposed by Reviewer#2 (L523).

475. Last instead of Finally.

AC: We changed it as proposed by Reviewer#2 (L525).

References. Some errors with author names (Farquhar was one) please check this carefully.

AC: As already mentioned in the response to Reviewer#1, we have corrected all the errors detected in the Reference list.

List of relevant changes made in the manuscript

- Following the reviewer’s suggestions, we have rewritten some sentences in the manuscript (see track changes’ version of the manuscript).
- We have added a link to the code of the model (L134-135):
<https://doi.org/10.6084/m9.figshare.5446435.v1>

- We have extended our discussion on the GNIP datasets quality (L421-436).

1 **Modelling tree-ring cellulose $\delta^{18}\text{O}$ variations of two temperature-sensitive tree**
2 **species from North and South America**

3

4

5 **Authors:**

6 Aliénor Lavergne¹, Fabio Gennaretti¹, Camille Risi², Valérie Daux³, Etienne Boucher⁴, Martine
7 M. Savard⁵, Maud Naulier⁶, Ricardo Villalba⁷, Christian Bégin⁵ and Joël Guiot¹

8

9 ¹Aix Marseille Université, CNRS, IRD, Collège de France, CEREGE, ECCOREV, Aix-en-
10 Provence, France

11 ²Laboratoire de Météorologie Dynamique, IPSL, UPMC, CNRS, Paris, France

12 ³Laboratoire des Sciences du Climat et de l'Environnement, CEA-CNRS-UVSQ, 91191 Gif-sur-
13 Yvette, France

14 ⁴Department of Geography and GEOTOP, Université du Québec à Montréal, Montréal, Canada

15 ⁵Geological Survey of Canada, Natural Resources Canada, 490 rue de la Couronne, QC,
16 G1K9A9, Canada

17 ⁶Institut de Radioprotection et de Sûreté Nucléaire (IRSN), PRP-ENV, SERIS/LRTE, Saint-Paul-
18 lez-Durance, France

19 ⁷Instituto Argentino de Nivología, Glaciología y Ciencias Ambientales, IANIGLA-CONICET,
20 Mendoza, Argentina

21

22 **Corresponding authors:** Aliénor Lavergne (alienor.lavergne@gmail.com) and Fabio Gennaretti
23 (gennaretti@cerege.fr)

24 Tel : +33 (0) 4 42 97 15 32

25 Centre Européen de Recherche et d'Enseignement en Géosciences

26 Technopôle de l'Arbois-Méditerranée

27 13545 Aix-en-Provence, FRANCE

28

29 **ABSTRACT**

30 | Oxygen isotopes in tree rings ($\delta^{18}\text{O}_{\text{TR}}$) are widely used to reconstruct past climates. However, the
31 complexity of climatic and biological processes controlling isotopic fractionation is not yet fully
32 understood. Here, we use the MAIDENiso model to decipher the variability of $\delta^{18}\text{O}_{\text{TR}}$ of two
33 temperature-sensitive species of relevant paleoclimatological interest (*Picea mariana* and
34 *Nothofagus pumilio*) and growing at cold high-latitudes in North and South America. In this first
35 modelling study on $\delta^{18}\text{O}_{\text{TR}}$ values in both northeastern Canada (53.86°N) and western Argentina
36 (41.10°S), we specifically aim at: 1) evaluating the predictive skill of MAIDENiso to simulate
37 $\delta^{18}\text{O}_{\text{TR}}$ values, 2) identifying the physical processes controlling $\delta^{18}\text{O}_{\text{TR}}$ by mechanistic modelling
38 and, 3) defining the origin of the temperature signal recorded in the two species. Although the
39 linear regression models used here to predict daily $\delta^{18}\text{O}$ of precipitation ($\delta^{18}\text{O}_{\text{P}}$) may need to be
40 improved in the future, the resulting daily $\delta^{18}\text{O}_{\text{P}}$ values adequately reproduce observed (from
41 weather stations) and simulated (by global circulation model) $\delta^{18}\text{O}_{\text{P}}$ series. The $\delta^{18}\text{O}_{\text{TR}}$ values of
42 the two species are correctly simulated using the $\delta^{18}\text{O}_{\text{P}}$ estimation as MAIDENiso input, although
43 some offset in mean $\delta^{18}\text{O}_{\text{TR}}$ levels is observed for the South American site. For both species, the
44 variability of $\delta^{18}\text{O}_{\text{TR}}$ series is more likely linked to the effect of temperature on isotopic
45 enrichment of the leaf water rather than on the isotopic composition of the source water. We
46 show that MAIDENiso is a powerful tool for investigating isotopic fractionation processes but
47 that the lack of a denser isotope-enabled monitoring network recording oxygen fractionation in
48 the soil-vegetation-atmosphere compartments limits our capacity to decipher the processes at
49 play. This study proves that the eco-physiological modelling of $\delta^{18}\text{O}_{\text{TR}}$ values is necessary to
50 interpret the recorded climate signal more reliably.

51

52 **Keywords:** MAIDENiso model, $\delta^{18}\text{O}$, tree-ring, *Nothofagus pumilio*, *Picea mariana*

53

54

55

Aliénor Lavergne 18/9/y 12:03

Supprimé: -

57 **1. INTRODUCTION**

58 Oxygen isotopes in tree rings ($\delta^{18}\text{O}_{\text{TR}}$) are increasingly used as indicators of past climatic
59 changes in temperate areas (Cernusak and English, 2015; Hartl-Meier et al., 2014; Saurer et al.,
60 2008). They have been widely used to reconstruct past atmospheric conditions such as air
61 temperature (Naulier et al., 2015), drought (Labuhn et al., 2016), precipitation amount (Rinne
62 et al., 2013), isotopic composition of precipitation (Danis et al., 2006), relative air humidity
63 (Wernicke et al., 2015), cloud cover (Shi et al., 2012), and even atmospheric circulation patterns
64 (Brienen et al., 2012). This diversity of climatic targets possibly reconstructed based on oxygen
65 isotopes hints at the challenge of understanding the complexity of the climatic and biological
66 processes that control isotopic fractionation of oxygen in trees (Treydte et al., 2014).
67 Uncertainties arise because different poorly measured factors influence $\delta^{18}\text{O}_{\text{TR}}$ values. Isotopic
68 signals in tree-rings cellulose are strongly influenced by isotopic signature of soil water taken up
69 by the roots and by evaporative and physiological processes occurring at the leaf level and during
70 downstream metabolism (Barbour et al., 2005; Gessler et al., 2014). Thus, a comprehensive
71 approach that embraces existing mechanistic understanding of the fractionation processes
72 involved is required.

73
74 Few isotopic process-based models have been developed to investigate the mechanistic rules
75 governing the $\delta^{18}\text{O}_{\text{TR}}$ variations (Guiot et al., 2014): the Pécelet-modified Craig-Gordon model
76 (Kahmen et al., 2011) and the Roden's model (Roden et al., 2000) are able to estimate, at a daily
77 time step, the $\delta^{18}\text{O}$ values of soil and xylem waters, and the isotopic fractionation occurring in the
78 leaves due to evapotranspiration. Versions of these models are integrated in more complete forest
79 ecophysiological models simulating the ensemble of forest water and carbon fluxes: (1)
80 MAIDEN (Modeling and Analysis In DENdroecology) (Gea-Izquierdo et al., 2015; Misson,
81 2004), which contains the isotopic module MAIDENiso (Danis et al., 2012) and (2) MUSICA
82 (Ogée et al., 2003, 2009). Both are accounting for important post-photosynthetic factors and are
83 able to link photosynthesis and carbohydrate allocation to stem growth.

84
85 In this paper, we use the MAIDENiso model to decipher the $\delta^{18}\text{O}_{\text{TR}}$ variability in American
86 temperature-sensitive species (*Picea mariana* in northeastern Canada and *Nothofagus pumilio* in
87 western Argentina). The selected sites are of special interest for paleoclimatology given that their

Unknown
Code de champ modifié

Unknown
Code de champ modifié

Unknown
Code de champ modifié

Unknown
Code de champ modifié

Unknown
Code de champ modifié

Unknown
Code de champ modifié

Unknown
Code de champ modifié

88 $\delta^{18}\text{O}_{\text{TR}}$ chronologies carry strong temperature signals. A summer temperature reconstruction was
89 already developed at the North American site (Gennaretti et al., 2017b; Naulier et al., 2015) and a
90 calibration study conducted at the South American one highlighted the strong potential of $\delta^{18}\text{O}_{\text{TR}}$
91 values to reflect variations in summer-autumn temperatures over a large region south of 38°S
92 (Lavergne et al., 2016). However, up to now, the climate- $\delta^{18}\text{O}_{\text{TR}}$ relationships were analysed
93 using a black box approach based on linear models. Here, we specifically aim at: 1) evaluating
94 the predictive skill of MAIDENiso to simulate $\delta^{18}\text{O}_{\text{TR}}$ values, 2) identifying the physical
95 processes controlling $\delta^{18}\text{O}_{\text{TR}}$ by mechanistic modelling and, 3) defining the origin of the
96 temperature signal recorded in the two species.

97

98 2. DATA AND METHODS

99 2.1. Sampling sites and tree-ring data

100 Two high-latitude American native species were studied here: 1) *Picea mariana* (Mill. B.S.P.;
101 black spruce), which is a conifer widely distributed over the American boreal forest (Viereck and
102 Johnston, 1990); and 2) *Nothofagus pumilio* (Poepp. et Endl. Krasser; lenga), which is an
103 **angiosperm** deciduous species dominating the high-elevation forests along the Patagonian Andes
104 from 35°S to 55°S (Donoso, 1981; Schlatter, 1994). We selected two sites of *P. mariana* in the
105 centre of the Quebec-Labrador Peninsula in northeastern Canada (L01 and L20; from 53°51'N-
106 72°24'W to 54°33'N-71°14'W, ~480 m elevation; see Gennaretti et al. (2014) and Naulier et al.
107 (2014) for details) and three sites of *N. pumilio* in northern Patagonia, western Argentina (NUB,
108 ALM and CHA; from 41°09'S-71°48'W to 41°15'S-71°17'W, 1270-1610 m elevation; see
109 Lavergne et al. (2016, 2017) for details). Climate in northeastern Canada is mostly continental
110 and subarctic with short, mild and wet summers and long, cold and dry winter. Total annual
111 precipitation averages 825 mm with up to 46% falling during the growing season in summer
112 (June to September) (Naulier et al., 2014). In western Argentina, precipitation is largely
113 concentrated from late fall to early spring (**May-November**) followed by a drier and mild period
114 during summer and early fall (**December-April**) (López Bernal et al., 2012).

115

116 Four trees per site were collected for both species. The selection of the samples and analytical
117 procedure for $\delta^{18}\text{O}_{\text{TR}}$ measurements were described in Lavergne et al. (2016) and Naulier et al.

Unknown

Code de champ modifié

Unknown

Code de champ modifié

Unknown

Code de champ modifié

Unknown

Code de champ modifié

Unknown

Code de champ modifié

Unknown

Code de champ modifié

Unknown

Code de champ modifié

Unknown

Code de champ modifié

Unknown

Code de champ modifié

118 (2014). The developed $\delta^{18}\text{O}_{\text{TR}}$ chronologies covered the 1950-2005 and 1952-2011 periods at the
119 northeastern Canadian and western Argentinian sites, respectively. [The chronologies that were](#)
120 [built for each species were significantly correlated between stands \(Figure 1\). This supported the](#)
121 [construction of a combined isotope chronology for both the northeastern Canada and western](#)
122 [Argentina sites.](#)

123 2.2. Modelling oxygen isotopes in tree-ring cellulose with MAIDENiso

125 MAIDENiso is a process-based model that can simulate in parallel phenological and
126 meteorological controls on photosynthetic activity and carbon allocation (Danis et al., 2012). It
127 explicitly allocates carbohydrates to different carbon pools (leaves, stem, storage and roots) on a
128 daily basis using phenological stage-dependent rules (see Gennaretti et al. (2017b) for details on
129 the construction of the main MAIDEN model). It also simulates the fractionation of carbon and
130 oxygen isotopes during growth processes. In particular, it estimates at a daily time step $\delta^{18}\text{O}$
131 values of soil water and xylem water, the isotopic fractionation occurring in the leaves due to
132 evapotranspiration and the biochemical fractionation during cellulose formation. It uses as input
133 daily maximum and minimum temperature ($^{\circ}\text{C}$), precipitation (cm/day), atmospheric CO_2
134 concentration (ppm) and $\delta^{18}\text{O}$ values of precipitation ($\delta^{18}\text{O}_{\text{P}}$ in ‰). [The code of the model can be](#)
135 [found here: <https://doi.org/10.6084/m9.figshare.5446435.v1>.](#)

137 In this study, the calculation of the daily $\delta^{18}\text{O}_{\text{TR}}$ in tree-ring cellulose (‰) is based on the (Danis
138 et al., 2012)'s formulation of the Craig-Gordon model (Craig and Gordon, 1965):

$$139 \delta^{18}\text{O}_{\text{TR}} = (1-f_o) \cdot [\epsilon^* + \epsilon_k \cdot (1-h_{\text{air}}) + h_{\text{air}} \cdot \delta^{18}\text{O}_{\text{V}} + (1-h_{\text{air}}) \cdot \delta^{18}\text{O}_{\text{XW}}] + f_o \cdot \delta^{18}\text{O}_{\text{XW}} + \epsilon_0 \quad (1)$$

140 This equation summarizes how $\delta^{18}\text{O}_{\text{TR}}$ is determined by:

- 141 (i) the $\delta^{18}\text{O}$ of the source (xylem) water ($\delta^{18}\text{O}_{\text{XW}}$), which is computed by averaging the
142 $\delta^{18}\text{O}_{\text{SW}}$ values of the different soil layers weighted by the volume of water taken up by
143 the roots in each layer. The isotopic effects of water mixing and soil evaporation on
144 the $\delta^{18}\text{O}_{\text{SW}}$ values of the different soil layers are computed by a mass and isotopic
145 balance (Danis et al., 2012). It is worth noting that no fractionation occurs during
146 water uptake by roots (Wershaw et al., 1966), neither during the transport of water
147 from the roots to the leaves.

Aliénor Lavergne 29/9/y 11:08

Supprimé: For each species, the chronologies obtained at the different stands being significantly inter-correlated (Figure 1), we chose to combine them and to develop one isotopic chronology for each of the two species.

Unknown

Code de champ modifié

Unknown

Code de champ modifié

Unknown

Code de champ modifié

Unknown

Code de champ modifié

Unknown

Code de champ modifié

- 153 (ii) the ^{18}O enrichment of the leaf water due to transpiration is described by
 154 $(\epsilon^* + \epsilon_k \cdot (1 - h_{\text{air}}) + h_{\text{air}} \cdot \delta^{18}\text{O}_V + (1 - h_{\text{air}}) \cdot \delta^{18}\text{O}_{\text{XW}})$ after (Craig and Gordon, 1965), where:
- 155 a. ϵ^* is the equilibrium fractionation due to the change of phase from liquid water to
 156 vapour at the leaf temperature (fixed at 21.4°C, the temperature threshold for
 157 maximum carbon assimilation, ϵ^* is 9.65‰ (Helliker and Richter, 2008)),
 - 158 b. ϵ_k is the kinetic fractionation due to the diffusion of vapour into unsaturated air
 159 through the stomata and the leaf boundary layer,
 - 160 c. h_{air} is the relative humidity of the evaporating air mass estimated from daily air
 161 temperature (T_{air} ; °C; mean of the maximum and minimum air temperatures), and
 162 the dew point temperature (T_r ; °C) (Running et al., 1987),
 - 163 d. $\delta^{18}\text{O}_V$ is the atmospheric water vapour calculated assuming a precipitation-vapour
 164 isotopic equilibrium (see below);
- 165 (iii) the biochemical fractionations (ϵ_0) due to oxygen exchange between carbonyl groups
 166 (C = O) in the organic molecules and water (DeNiro and Epstein, 1979; Farquhar et
 167 al., 1998).
- 168 (iv) the dampening factor f_0 reflecting the exchange of the oxygen atoms between sucrose
 169 and xylem water during cellulose synthesis in the xylem cells of tree rings.

170 As previously evoked (i), $\delta^{18}\text{O}_{\text{XW}}$ of Eq. 1 depends on $\delta^{18}\text{O}_{\text{SW}}$ and thus on $\delta^{18}\text{O}_P$ values. However,
 171 long continuous time series of $\delta^{18}\text{O}_P$ are not available in the studied area (see [http://www-](http://www-naweb.iaea.org/naweb/ih/IHS_resources_gnip.html)
 172 [naweb.iaea.org/naweb/ih/IHS_resources_gnip.html](http://www-naweb.iaea.org/naweb/ih/IHS_resources_gnip.html)). Here, we tested the impact of using two
 173 different methods for deriving $\delta^{18}\text{O}_P$ time series.

174 First, a linear model was used to estimate the daily values of $\delta^{18}\text{O}_P$ and subsequently $\delta^{18}\text{O}_V$ based
 175 on the primary drivers of their temporal variability (Dansgaard, 1964; Horita and Wesolowski,
 176 1994), that are air temperature (T_{air} ; °C) and precipitation at the corresponding site (P ; mm):

$$\delta^{18}\text{O}_P = a \cdot T_{\text{air}} + b \cdot P + c \quad (2)$$

$$\delta^{18}\text{O}_V = \delta^{18}\text{O}_P - \epsilon^*_{T_{\text{air}}} \quad (3)$$

179 with $\epsilon^*_{T_{\text{air}}}$ the fractionation due to the change of phase from liquid water to vapour at the mean air
 180 temperature. The coefficients a and b were allowed to vary over a plausible range (or prior range)
 181 in the calibration process together with other MAIDENiso parameters, while coefficient c was

Unknown
Code de champ modifié

Unknown
Code de champ modifié

Unknown
Code de champ modifié

Unknown
Code de champ modifié

Aliénor Lavergne 29/9/y 11:12
Supprimé: ly

Unknown
Code de champ modifié

183 fixed to a likely value (see Table 1 and section 2.4). This estimated set of data is referred in the
184 following as the estimated $\delta^{18}\text{O}_\text{P}$ dataset.

185 Second, we run the model with the series of the daily $\delta^{18}\text{O}_\text{P}$ derived from two general circulation
186 models (GCM) with different spatial resolutions and enough available data at our site locations:
187 1) the MUGCM model (Noone and Simmonds, 2002) forced by varying sea surface temperature
188 (SST) from the HadISST data set for the 1950-2003 period ($2^\circ \times 2^\circ$ resolution; extracted at
189 <http://paos.colorado.edu/~dcn/SWING/database.php>; hereafter referred as MUGCM $\delta^{18}\text{O}_\text{P}$
190 dataset), and 2) the [Laboratoire de Météorologie Dynamique Zoom \(LMDZ5A\)](#) model (Hourdin
191 et al., 2013; Risi et al., 2010) with the horizontal winds guided by those of the [National Centers
192 for Environmental Protection - 20th Century Reanalysis \(NCEP20\)](#) for the 1950-2008 period
193 (Compo et al., 2011) ($2.5^\circ \times 3.75^\circ$ resolution; hereafter referred as LMDZ-NCEP20 $\delta^{18}\text{O}_\text{P}$ dataset).

194
195 The final $\delta^{18}\text{O}_\text{TR}$ time series are the annual average of the $\delta^{18}\text{O}_\text{TR}$ daily values (Eq. 1) weighted by
196 the daily simulated stand Gross Primary Production (GPP), assuming a proportional allocation of
197 carbon to the trunk. For the northeastern Canadian sites, the GPP simulated by MAIDENiso was
198 optimized using observations from an eddy covariance station (see Gennaretti et al. (2017a)).

199 Unfortunately, such observations were not available for *N. pumilio*, and therefore the
200 parameterization obtained for the GPP of *P. mariana* was also used for the western Argentinian
201 sites but constraining the simulations with phenological observations extracted from the
202 literature. For example, to respect the annual cycle of the leaf area index (LAI) for *N. pumilio*
203 (Magnin et al., 2014; Rusch, 1993), we used in MAIDENiso a seasonal LAI annual cycle with a
204 development of leaves (LAI increase) between October and November, a maximum LAI (set at 5
205 leaf area/ground area) from November to April, a decreasing LAI (leaf fall) between April and
206 May, and finally a leafless period (null LAI) from June to September (Magnin et al., 2014;
207 Rusch, 1993). Furthermore, based on the finding that $\delta^{18}\text{O}_\text{TR}$ annual time series were more
208 correlated to climate variables of specific months of the growing season (Lavergne et al., 2016),
209 we also computed $\delta^{18}\text{O}_\text{TR}$ annual values by weighting the $\delta^{18}\text{O}_\text{TR}$ daily values (Eq. 1) with
210 synthetic GPP time series maximizing the correspondence between observations and simulations.

211

212 2.3. Meteorological and atmospheric CO₂ data

Aliénor Lavergne 29/9/y 11:12
Supprimé: ly

Unknown
Code de champ modifié

Unknown
Code de champ modifié

Unknown
Code de champ modifié

Aliénor Lavergne 29/9/y 11:20
Supprimé: NCEP20 reanalysis

Unknown
Code de champ modifié

Unknown
Code de champ modifié

Unknown
Code de champ modifié

Unknown
Code de champ modifié

Unknown
Code de champ modifié

215 At the western Argentinian sites, we did not have long daily records of observed climate data.
216 Therefore, daily minimum–maximum temperature and precipitation data were derived from the
217 20th Century Reanalysis V2c (Compo et al., 2011) provided by the NOAA/OAR/ESRL ($2^{\circ} \times 2^{\circ}$
218 resolution, https://www.esrl.noaa.gov/psd/data/gridded/data.20thC_ReanV2c.html), which is one
219 of the few reanalysis products covering entirely the 20th century. The temperature daily time
220 series of the reanalysis were corrected in order to respect the monthly mean values detected at
221 Bariloche, the nearest meteorological station from our sampling sites (~48 km from the sites,
222 $41^{\circ}12' \text{ S} - 71^{\circ}12' \text{ W}$, 840 m asl; Servicio Meteorológico Nacional, Argentina). The resulting
223 maximum and minimum temperature series, covering the 1952-2011 period, fit well with the
224 daily local temperature data from La Almohadilla (ALM) site ($41^{\circ}11' \text{ S}$, $71^{\circ}47' \text{ W}$, 1410 m asl;
225 data measured by dataloggers and provided by IANIGLA) available over the 2002-2012 period (r
226 = 0.74, $p < 0.001$; Figure SM1). For the northeastern Canadian sites, climate data were obtained
227 from the gridded interpolated Canadian database of daily minimum–maximum temperature and
228 precipitation covering the 1950-2005 studied period ($0.08^{\circ} \times 0.08^{\circ}$ resolution, (Hutchinson et al.,
229 2009); <http://cfs.nrcan.gc.ca/projects/3/4>). In addition to these data we also used modelled daily
230 data from the GCMs described above for both the western Argentinian and northeastern Canadian
231 sites (see Table 2 with the input data used for each tested configuration).

232
233 Data on the atmospheric CO_2 concentration were derived from the Mauna Loa station over the
234 1958-2012 period (Keeling et al. (1976); <http://www.esrl.noaa.gov/gmd/ccgg/trends/>). For the
235 years 1950-1957, we extrapolated atmospheric CO_2 data using the trend and seasonal cycle
236 observed in the observations over the subsequent 10-years period (1958-1967).

237 2.4. Estimation of parameters influencing $\delta^{18}\text{O}_{\text{TR}}$

239 We used a Bayesian method for the simultaneous calibration of the various MAIDENiso
240 parameters specific to the study species and site. A set of 50 plausible blocks of parameters
241 (posterior values) was selected according to the method described in Gennaretti et al. (2017a)
242 using Markov Chain Monte Carlo (MCMC) sampling (Table 1). The following prior plausible
243 ranges were considered:

244 1) the prior ranges of the a and b coefficients in the equation of the daily $\delta^{18}\text{O}_{\text{P}}$ (Eq. 2) were
245 selected in order to get $\delta^{18}\text{O}_{\text{P}}$ values for each site consistent with the measured monthly local

Unknown
Code de champ modifié

Unknown
Code de champ modifié

Unknown
Code de champ modifié

Unknown
Code de champ modifié

Unknown
Code de champ modifié

Aliénor Lavergne 18/9/y 12:06
Supprimé: for both the western Argentinian and northeastern Canadian sites

Unknown
Code de champ modifié

Aliénor Lavergne 18/9/y 12:07
Supprimé: years

Unknown
Code de champ modifié

249 values from the nearest stations of the Global Network of Isotopes in Precipitation (GNIP), and
250 with the simulated daily values from the LMDZ-NCEP20 model and from the MUGCM model
251 (see Table 1),

252 2) the range for the biochemical fractionation factor ϵ_0 was chosen between 24‰ and 30‰
253 (+27±3‰ after DeNiro and Epstein (1981); Sternberg (1989); Yakir and DeNiro (1990)),

254 3) the range for the kinetic fractionation ϵ_k , which has been set to 26.5‰ in Farquhar et al. (1989)
255 but that can vary over larger ranges (Buhay et al., 1996), was taken between 10‰ and 30‰ here,

256 4) the range for the dampening factor f_0 was allowed to vary between 0.3 and 0.5 following
257 Saurer et al. (1997).

258

259 We tested the sensitivity of the MAIDENiso model to the calibrated parameters by modifying
260 them within their respective prior calibration range. To control the robustness of the calibrated
261 parameters, we performed the calibration of these parameters over two equal length intervals
262 (1950-1977 and 1978-2005 for *P. mariana*; 1952-1981 and 1982-2011 for *N. pumilio*) keeping
263 the second half for independent validation of the parameters estimates. Once the model was
264 calibrated for the two species, the MAIDENiso's performance to simulate *P. mariana* and *N.*
265 *pumilio* $\delta^{18}\text{O}_{\text{TR}}$ interannual data was evaluated using the correlation coefficients (r) and the root
266 mean square errors (RMSE) between observed and simulated values. [This is a standard approach](#)
267 [to evaluate how well a mechanistic model is simulating \$\delta^{18}\text{O}_{\text{TR}}\$ variations \(e.g. Danis et al., 2012;](#)
268 [Lorrey et al., 2016\).](#)

270 **2.5. Disentangling leaf-level fractionation processes and source water influences on** 271 **$\delta^{18}\text{O}_{\text{TR}}$ signature**

272 To define the relative contributions to the $\delta^{18}\text{O}_{\text{TR}}$ signature of the isotopic signal of the source
273 water (xylem water) and of the fractionation processes due to transpiration taking place in the
274 leaves, we designed two experimental simulations with MAIDENiso based on Eq. 1:

275 1) to quantify the influence of the variability of the isotopic composition of the xylem water
276 on $\delta^{18}\text{O}_{\text{TR}}$, we compared the reference simulations to those where the relative humidity
277 (h_{air}) and the isotopic composition of atmospheric vapour ($\delta^{18}\text{O}_{\text{V}}$) were assumed to be
278 constant. The constant values for h_{air} and $\delta^{18}\text{O}_{\text{V}}$ were defined as the averages of the
279 respective MAIDENiso outputs ($h_{\text{air}} = 0.62$ and 0.9 , and, $\delta^{18}\text{O}_{\text{V}} = -26.28\text{‰}$ and -17.34‰ ,

Unknown
Code de champ modifié

Unknown
Code de champ modifié

Unknown
Code de champ modifié

Unknown
Code de champ modifié

Unknown
Code de champ modifié

280 | respectively for northeastern Canada and western Argentina; the XW_v source experiment
281 | simulation hereafter),

282 | 2) to quantify the influence of the isotopic enrichment of the leaf water due to transpiration
283 | on $\delta^{18}\text{O}_{\text{TR}}$, we compared the reference simulations to those where the $\delta^{18}\text{O}_{\text{XW}}$ series were
284 | assumed to be constant. The constant value for $\delta^{18}\text{O}_{\text{XW}}$ was estimated as the average of
285 | the $\delta^{18}\text{O}_{\text{XW}}$ MAIDENiso outputs ($\delta^{18}\text{O}_{\text{XW}} = -13.81\text{‰}$ and -7.03‰ , respectively for
286 | northeastern Canada and western Argentina; the Leaf water enrichment driven experiment
287 | simulation hereafter).

288 | Comparison between the experimental and reference simulations (i.e. using the optimal values of
289 | the parameters) was achieved through the calculation of the coefficient of determination (R^2).

290

291 | 3. RESULTS

292 | 3.1. Estimated versus modelled and observed $\delta^{18}\text{O}_{\text{P}}$ values

293 | The modelled $\delta^{18}\text{O}_{\text{P}}$ series from the GCM models are similar to the GNIP datasets, with mean
294 | values ranging from -12‰ to -8‰ over June-September in northeastern Canada (Figure SM2A)
295 | and from -7‰ to -3‰ over December-April at the western Argentinian sites (Figure SM2B). In
296 | general, $\delta^{18}\text{O}_{\text{P}}$ series from LMDZ-NCEP20 model in western Argentina are slightly displaced
297 | toward higher values ($+1\text{‰}$) in comparison with the GNIP and MUGCM data. The estimated
298 | $\delta^{18}\text{O}_{\text{P}}$ values based on plausible values of coefficients a and b agree well with those of the models
299 | and observations in northeastern Canada. For the western Argentinian sites, they are 2-3‰ lower
300 | from April to October, i.e. late spring-early autumn (Figure SM2).

301

302 | 3.2. Sensitivity of the model to the calibrated parameters

303 | Most of the calibrated parameters have an influence on the correlations between observed and
304 | simulated $\delta^{18}\text{O}_{\text{TR}}$ series and/or on the mean levels of the simulated series (Figure 2). The
305 | temperature and precipitation dependences of $\delta^{18}\text{O}_{\text{P}}$ values (respectively a and b coefficients)
306 | have the strongest influence on correlations. Increasing a and b values increase the mean $\delta^{18}\text{O}_{\text{TR}}$
307 | levels, more strongly in western Argentina than in northeastern Canada (Figure 2). Changes in
308 | the dampening factor (f_o) and in the biochemical fractionation (ϵ_o) have almost no effect on
309 | correlation, but their increase induces significant decrease of the mean levels of $\delta^{18}\text{O}_{\text{TR}}$ series.

Aliénor Lavergne 29/9/y 11:53

Supprimé: _

Aliénor Lavergne 29/9/y 11:53

Supprimé: _

Aliénor Lavergne 29/9/y 11:53

Supprimé: _

Aliénor Lavergne 29/9/y 11:53

Supprimé: _

Aliénor Lavergne 18/9/y 12:09

Supprimé: most

315 Finally, increasing the kinetic fractionation (ϵ_k) leads to lower correlations and to higher mean
316 levels of $\delta^{18}\text{O}_{\text{TR}}$ (Figure 2).

317

318 3.3. MAIDENiso performance in reproducing observed $\delta^{18}\text{O}_{\text{TR}}$ series

319 Split-period verifications of the calibrated relationships for *P. mariana* and *N. pumilio* when
320 using estimated $\delta^{18}\text{O}_p$ series from Eq. 2 indicate that the calibration over either the first half or the
321 second half periods provide similar posterior densities of the calibrated parameters than the ones
322 obtained when calibrating over the whole periods (Figure SM3). One exception is observed in the
323 calibration of coefficient *a* in northeastern Canada over the two half periods, where the posterior
324 densities of *a* are different from the one obtained by calibrating over the entire period. Over the
325 entire periods, observed and simulated $\delta^{18}\text{O}_{\text{TR}}$ series are significantly correlated in northeastern
326 Canada ($r = 0.56$, $p < 0.01$ and $\text{RMSE} = 0.67$; Figure 3A) and in western Argentina ($r = 0.48$, $p <$
327 0.01 and $\text{RMSE} = 0.63$; Figure 3C). The correlation between observed and simulated $\delta^{18}\text{O}_{\text{TR}}$
328 series are slightly improved when we used synthetic daily GPP ($r = 0.62$ and $r = 0.52$, $p < 0.01$,
329 respectively for northeastern Canada and western Argentina; Figure 3B and 3D). It is worth
330 noting that the mean levels of the simulated $\delta^{18}\text{O}_{\text{TR}}$ series for the Argentinian sites are lower than
331 those of the observations (offset of around -2.5% ; Figure SM4). The series were therefore
332 corrected to respect the mean values detected in the observations (Figure 3C and 3D). In contrast,
333 the correlations between observation and simulation considerably decrease when we used
334 modelled $\delta^{18}\text{O}_p$ from MUGCM models or LMDZ-NCEP20 reanalysis data. They only reach
335 $r = 0.13$ ($p > 0.05$) to 0.23 ($p < 0.05$) in northeastern Canada and $r = 0.23$ to 0.26 ($p < 0.05$) in
336 western Argentina, respectively (Figure 4).

337

338 3.4. Influence of source water and leaf water isotopic enrichment to the $\delta^{18}\text{O}_{\text{TR}}$ signature

339 The relative contributions to the $\delta^{18}\text{O}_{\text{TR}}$ signature of the isotopic signal of the source (xylem)
340 water and of the ^{18}O enrichment of the leaf water due to transpiration were investigated. In both
341 regions, the Leaf water enrichment experimental simulations are more highly related to the
342 reference simulations (R^2 centred on 0.9 and 0.95, respectively for northeastern Canada and
343 western Argentina; Figure 5) than are the XW source simulations (R^2 centred on 0.65 and 0.8,
344 respectively for northeastern Canada and western Argentina). This suggests that, with the model,
345 the variability of $\delta^{18}\text{O}_{\text{XW}}$ has a weaker influence on $\delta^{18}\text{O}_{\text{TR}}$ variations than the changes of the leaf

Aliénor Lavergne 29/9/y 12:21

Supprimé: _

Aliénor Lavergne 29/9/y 12:21

Supprimé: _

Aliénor Lavergne 18/9/y 12:09

Supprimé: one

Aliénor Lavergne 29/9/y 12:21

Supprimé: _

Aliénor Lavergne 18/9/y 12:10

Supprimé: ones

351 water isotopic enrichment do. Notably, *P. mariana* in northeastern Canada appears to be more
352 sensitive to both influences than *N. pumilio* in western Argentina (Figure 5).

353

354 4. DISCUSSION

355 4.1. Precipitation $\delta^{18}\text{O}_P$ variations and estimation

356 Although the regression models used to predict daily $\delta^{18}\text{O}_P$ values are likely too simplistic, the
357 resultant monthly averaged values adequately reproduce the distribution of the observed (from
358 GNIP stations) and modelled (by GCMs) monthly $\delta^{18}\text{O}_P$ series in northeastern Canada. In
359 western Argentina, the distribution of monthly $\delta^{18}\text{O}_P$ values is also well reproduced but the
360 amplitude of variation of the predicted values is too high, leading to simulated values lower than
361 the measured ones during the colder months. The temporal $\delta^{18}\text{O}_P$ variations are positively related
362 to air temperature given the positive coefficient a . In agreement with the simple Rayleigh
363 distillation model (Dansgaard, 1964), as air temperature decreases, the specific humidity at
364 saturation decreases, and water vapour condenses. H_2^{18}O condenses preferentially, the residual
365 water vapour gets more and more depleted as condensation proceeds. Consequently, in the
366 Tropics, the $^{18}\text{O}/^{16}\text{O}$ ratio in the meteoric water has been observed to decrease with increasing
367 amount of precipitation and/or relative humidity (Rozanski et al., 1993). In extra-tropical regions,
368 $\delta^{18}\text{O}_P$ may also correlate with precipitation amount (negative coefficient b), since both variables
369 depend on the meteorological conditions.

370 The results of the linear regressions show comparatively lower influence of precipitation on
371 $\delta^{18}\text{O}_P$ in western Argentina than in northeastern Canada (Table 1). This suggests that the imprint
372 of the precipitation amount on $\delta^{18}\text{O}_P$ in western Argentina is low and that $\delta^{18}\text{O}_P$ variations are
373 mainly controlled by seasonal changes in temperature, which is in agreement with previous work
374 (Rozanski et al., 1995). However, due to the strong west-to-east precipitation gradient in this
375 region (orographic rain shadow), large $\delta^{18}\text{O}_P$ variations occur over short distances (Rozanski et
376 al., 1995; Smith and Evans, 2007; Stern and Blisniuk, 2002). Therefore, the daily precipitation
377 dataset extracted from the gridded reanalysis data, which has a low spatial resolution (>200 km),
378 may not represent the daily variations in precipitation at a local scale faithfully. Therefore, the
379 model may underestimate the contribution of precipitation on $\delta^{18}\text{O}_P$ variability in this particular
380 area.

381

Aliénor Lavergne 29/9/y 12:24

Supprimé: Caution should be made here since these results are limited upstream by the performance of the regressions. ... [1]

Unknown

Code de champ modifié

Aliénor Lavergne 2/10/y 14:59

Supprimé: In

Aliénor Lavergne 2/10/y 14:59

Supprimé: relative abundance of

Aliénor Lavergne 2/10/y 15:00

Supprimé: leading to a decrease in $^{18}\text{O}/^{16}\text{O}$ ratio in a high amount of precipitated water

Unknown

Code de champ modifié

Unknown

Code de champ modifié

Unknown

Code de champ modifié

390 | In contrast, in northeast Canada, both temperature and precipitation amount equally control the
391 $\delta^{18}\text{O}_\text{P}$ variations. The high amount of precipitation falling in summer (~46%) should have a
392 strong effect and decrease the $\delta^{18}\text{O}_\text{P}$ values in the condensed water, while high temperatures
393 counteract this effect by increasing this ratio. Before reaching northeastern Canada, the air
394 masses pushed by the dominant westerly winds discharge most of their humidity over the land,
395 leading to a depleted $\delta^{18}\text{O}_\text{P}$ signal at our sites (for the same reason, $\delta^{18}\text{O}_\text{TR}$ values at L20, which is
396 located 110 km North-East of L01, are ~1‰ lower). Moreover, the $\delta^{18}\text{O}_\text{P}$ signal in the Canadian
397 sites is comparatively more depleted than in the Argentinian sites, because of their higher
398 latitude. It is worth noting that the resolution of the gridded meteorological dataset used for the
399 Canadian sites is relatively high (~10 km), which means that the local processes are likely well
400 represented.

Aliénor Lavergne 29/9/y 12:26

Supprimé: Contrastingly

Aliénor Lavergne 18/9/y 12:20

Supprimé: em

Aliénor Lavergne 18/9/y 12:15

Supprimé: Interestingly

Aliénor Lavergne 2/10/y 14:46

Supprimé:

Aliénor Lavergne 2/10/y 14:46

Supprimé: northeastern

Aliénor Lavergne 2/10/y 14:46

Supprimé: western

Aliénor Lavergne 2/10/y 14:47

Supprimé: here

402 4.2. Relative performance in modelling $\delta^{18}\text{O}_\text{TR}$ values

403 The simulated $\delta^{18}\text{O}_\text{TR}$ series based on daily $\delta^{18}\text{O}_\text{P}$ estimation from the regression models
404 reproduce the observations better than the ones based on $\delta^{18}\text{O}_\text{P}$ values derived from GCMs
405 (Figure 4). This is in part due to the greater number of parameters to optimize, as the calibration
406 process can more easily find a solution that fits the observations better. This may however reflect
407 error compensations especially in western Argentina where the estimated annual variability of
408 $\delta^{18}\text{O}_\text{P}$ is too large. Conversely in northeastern Canada, the annual variations of $\delta^{18}\text{O}_\text{P}$ that are
409 estimated, simulated by GCMs and observed are in good agreement (Figure SM2). Although
410 isotope-enabled atmospheric global models can reproduce the mean annual precipitation isotopic
411 values and seasonality for many areas (Risi et al., 2010), results at specific sites, especially in
412 mountainous regions such as at our western Argentinian site, can be less accurate (Figure SM2;
413 see the offset between GNIP stations and LMDZ-NCEP20). Ideally, daily $\delta^{18}\text{O}_\text{P}$ long-term
414 records from meteorological stations in the study region should be used as an input of
415 MAIDENiso. Simulations from high-resolution regional circulation models, such as REMOiso
416 which has a $0.5^\circ \times 0.5^\circ$ (~55 km) horizontal resolution (Insel et al., 2013; Sturm et al., 2007,
417 2005), may produce reliable local $\delta^{18}\text{O}_\text{P}$ values. Such dataset has proven to be quite helpful with
418 MAIDENiso in the Fontainebleau forest (France) (Danis et al., 2012). However, up to now,
419 measured or REMOiso $\delta^{18}\text{O}_\text{P}$ datasets in our regions of study do not exist, which is the case for
420 most regions of the world. Moreover, early data (1970-80s) from GNIP stations may have been

Aliénor Lavergne 29/9/y 12:32

Supprimé: Although isotope-enabled atmospheric global models reproduce reasonably well the global distribution of the mean annual isotope contents of the modern precipitation and their seasonality

Unknown

Code de champ modifié

Unknown

Code de champ modifié

Unknown

Code de champ modifié

432 compromised by pan evaporation and therefore isotopic enrichment. Therefore, we recommend
433 that daily GNIP stations are set up in various forested ecosystems, that an effort is accomplished
434 to homogenize older GNIP time series, and that high resolution simulations of $\delta^{18}\text{O}_p$ are
435 performed in wider regions.

436
437 The modelling of $\delta^{18}\text{O}_{\text{TR}}$ values based on the estimation of $\delta^{18}\text{O}_p$ is relatively more accurate for
438 northeastern Canada than for western Argentina (Figure 3). As the mean levels of the measured
439 $\delta^{18}\text{O}_{\text{TR}}$ values are high at the western Argentinian sites (mean value of about 30‰), the Bayesian
440 optimization tends to increase the biochemical (ϵ_0) and kinetic (ϵ_k) fractionations as well as the
441 coefficient a , while reducing the dampening factor (f_0) to reach more representative mean levels
442 of the $\delta^{18}\text{O}_{\text{TR}}$ simulation. But still, these levels are too low in comparison with the observations
443 (about 2.5‰ lower; Figure SM4). When the posterior value of a calibrated parameter is limited to
444 the upper bound of the prior range of plausible values, as it is the case at the western Argentinian
445 sites for a , b and ϵ_0 (Figure SM3), it means that either the prior range is too narrow, or the model
446 is inadequate, or some important process is not considered in the model. Here, the estimation of
447 the prior ranges of both coefficients a and b were based on observed (GNIP stations) and
448 simulated (GCMs) $\delta^{18}\text{O}_p$ values. Therefore, we expect their respective ranges to be consistent
449 with local processes. When the prior range of a is extended to higher values in the optimization
450 process, observed and simulated $\delta^{18}\text{O}_{\text{TR}}$ mean levels in western Argentina are better matching.
451 However, in this case, the distribution of $\delta^{18}\text{O}_p$ values is shifted toward higher values, advocating
452 for unrealistic estimated $\delta^{18}\text{O}_p$ variations.

453 One other possibility is that the prior range of ϵ_0 is too narrow. In accordance with DeNiro and
454 Epstein (1981), Sternberg (1989) and Yakir and DeNiro (1990), the biochemical fractionation ϵ_0
455 is assumed here to be lower than 30‰. However, a recent study has demonstrated that this
456 parameter, nearly constant between 20 to 30°C, increases at lower temperatures to values of 31‰
457 (Sternberg and Ellsworth, 2011). During the growing season, maximum temperatures can reach
458 20°C in western Argentina and 30°C in northeastern Canada, which suggests that the high mean
459 $\delta^{18}\text{O}_{\text{TR}}$ levels in *N. pumilio* may be due to biochemical fractionation higher than 30‰ due to
460 temperature generally lower than 20°C. However, when the prior range of ϵ_0 is extended to 31‰
461 in the optimization process, the mean $\delta^{18}\text{O}_{\text{TR}}$ levels of *N. pumilio* are still too low in comparison
462 with the observations. These results advocate for the existence of other processes, which can

Unknown
Code de champ modifié

Unknown
Code de champ modifié

463 explain this offset in mean levels in Argentina. For example, higher soil water evaporation than
464 modelled by MAIDENiso should lead to less negative $\delta^{18}\text{O}_{\text{SW}}$ (and therefore $\delta^{18}\text{O}_{\text{XW}}$), which
465 could explain the high mean levels of $\delta^{18}\text{O}_{\text{TR}}$ in Argentina. Caution should be exercised with such
466 an interpretation since other species living in similar conditions as *N. pumilio* in western
467 Argentina show comparatively lower mean $\delta^{18}\text{O}_{\text{TR}}$ levels than *N. pumilio* (i.e., *Fitzroya*
468 *cupressoides*; see Lavergne et al. (2016)). The ongoing monitoring and evaluation of isotopic
469 processes based on synchronous measurements of vapour, precipitation, soil water and xylem
470 water will certainly help understanding the high mean levels observed in Argentina, and
471 increasing the representation of the involved processes in MAIDENiso.

472

473 The better fit between observed and simulated $\delta^{18}\text{O}_{\text{TR}}$ values obtained with specific forms of
474 synthetic distributions of daily GPP for northeastern Canada and western Argentina (Figure 3)
475 suggests differential limiting factors in the two regions. The synthetic bimodal distribution of
476 daily GPP with maxima in spring and autumn, as simulated in western Argentina, is often
477 observed in a diversity of ecosystems such as in the Mediterranean environments (Baldocchi et
478 al., 2010; Gea-Izquierdo et al., 2015). After the activation of the photosynthesis in early spring,
479 increasing temperatures tend to be optimal for tree growth. However, in a modelling study,
480 Lavergne et al. (2015) have shown that the influence of temperature on *N. pumilio*'s growth
481 becomes negative once a temperature threshold (soil moisture) is exceeded. Therefore, we
482 assume that after reaching a threshold of temperature and soil moisture summer conditions, tree
483 growth is inhibited, leading to a decrease of primary productivity. However, when temperature
484 starts to decline and soil water supply tends to increase with increasing precipitation events, tree
485 growth increases again until the end of the growing season. In contrast, because precipitation is
486 more abundant in summer (June to September) in northeastern Canada (Naulier et al., 2014), high
487 summer temperatures should be always beneficial to tree-growth if enough soil water is available.
488 Therefore, in agreement with GPP-derived eddy covariance data from the Fluxnet network (see
489 Gennaretti et al. (2017a)), a better fit between observations and simulations is observed when
490 using a unimodal rather than a bimodal GPP distribution. Monitoring of tree physiology,
491 environmental conditions and wood cell formation will provide a more detailed representation of
492 the complex biological and ecological processes operating in Patagonia, allowing us to run the
493 MAIDENiso model with better constraints.

Unknown
Code de champ modifié

Unknown
Code de champ modifié

Unknown
Code de champ modifié

Aliénor Lavergne 18/9/y 12:22
Supprimé: not favoured

Unknown
Code de champ modifié

Unknown
Code de champ modifié

495

496 4.3. What is the main origin of the temperature signal recorded in $\delta^{18}\text{O}_{\text{TR}}$?

497 The investigation of the relative contributions of the isotopic composition of the source (xylem)
498 water and of the ^{18}O enrichment of the leaf water by transpiration on the simulated $\delta^{18}\text{O}_{\text{TR}}$ reveals
499 that the variability of the former has a weaker influence on $\delta^{18}\text{O}_{\text{TR}}$ variations than that of the
500 latter in North and South America. Therefore, the temperature signal recorded in $\delta^{18}\text{O}_{\text{TR}}$ series
501 more likely reflects the effect of temperature on isotopic enrichment of the leaf water rather than
502 on the isotopic composition of the source water. At the leaf-level, air temperature has a strong
503 effect on the relative humidity and therefore on the vapour pressure deficit (VPD), i.e. the
504 difference between the saturation vapour pressure and the actual vapour pressure, which
505 modulates the transpiration (Barbour, 2007). Thus, the imprint of the ambient air temperature on
506 the fractionation processes occurring during transpiration is preferentially recorded in the tree
507 rings of the two species. Furthermore, both the isotopic signature of the xylem water and of the
508 fractionation processes occurring at the evaporation sites of the leaves have comparatively higher
509 influence on $\delta^{18}\text{O}_{\text{TR}}$ in *P. mariana* than in *N. pumilio*. This is probably due to the lower amplitude
510 of the day-by-day variations of the relative humidity in western Argentina (SD = 5%) versus in
511 northeastern Canada (SD = 16%) that translates into a weaker influence of h_{air} variations and
512 therefore of leaf-level isotopic fractionation processes on $\delta^{18}\text{O}_{\text{TR}}$ values in western Argentina
513 than in northeastern Canada. These results highlight the potential of MAIDENiso model to better
514 refine the origin of the climatic signal recorded in the oxygen isotopic signature in the tree-rings
515 of different species.

516

517 5. CONCLUSION

518 Here, by using MAIDENiso model, we provided a mechanistic overview of the climatic and
519 biological processes controlling oxygen isotopic fractionation in two American temperature-
520 sensitive tree species. First, we have shown that using regression-based rather than model-based
521 $\delta^{18}\text{O}_{\text{P}}$ estimates as inputs increases the predictive skills of our simulations, although this may be
522 at the price of error compensations. Second, our study reveals that the variability of the isotopic
523 composition of the source (xylem) water has a weaker influence on $\delta^{18}\text{O}_{\text{TR}}$ variations than that of
524 the ^{18}O enrichment of the leaf water by transpiration. Last, these findings suggest that the imprint

Unknown

Code de champ modifié

Aliénor Lavergne 18/9/y 12:23

Supprimé: -

Aliénor Lavergne 29/9/y 12:43

Supprimé: ly

Aliénor Lavergne 29/9/y 12:43

Supprimé: ly

Aliénor Lavergne 29/9/y 12:43

Supprimé: Finally

529 of temperature recorded in $\delta^{18}\text{O}_{\text{TR}}$ of the two species is likely related to the effect of temperature
530 on isotopic enrichment of the leaf water. The isotopic monitoring of water within the soil-
531 vegetation-atmosphere compartments in future work will certainly provide the input and control
532 data necessary to better constrain MAIDENiso. Our study demonstrates that the eco-
533 physiological modelling of $\delta^{18}\text{O}_{\text{TR}}$ values is necessary and likely the only approach to accurately
534 interpret the recorded climate signal. Based on the calibrations of MAIDENiso presented here,
535 the next step involves inverse modelling approaches to perform paleoclimatic reconstructions in
536 North and South America that are less biased by the complex and nonlinear interactions between
537 climate, CO_2 concentrations and tree growth as recommended by Boucher et al. (2014).

538

539 ACKNOWLEDGMENTS

540 A.L. has been supported by a Research associate/Lecturer position at the Aix-Marseille
541 University (France). F.G. has received funding from the European Union's Horizon 2020
542 research and innovation program under the Marie Skłodowska-Curie grant agreement No
543 656896. We acknowledge all data providers: the Instituto Argentino de Nivología, Glaciología y
544 Ciencias Ambientales (IANIGLA, Argentina) for providing the daily temperature data from La
545 Almohadilla site; the National Meteorological Service from Argentina for providing the monthly
546 temperature data from Bariloche meteorological station (Argentina); the Department of Natural
547 Resources Canada for providing the daily climatic data used for Quebec; the US Department of
548 Energy, Office of Science Biological and Environmental Research (BER) and the National
549 Oceanic and Atmospheric Administration Climate Program Office for providing the daily
550 climatic data used for Argentina; and the SWING project for providing the daily $\delta^{18}\text{O}_p$ data from
551 MUGCM model.

552

553

References

554 Baldocchi, D. D., Ma, S., Rambal, S., Misson, L., Ourcival, J. M., Limousin, J. M., Pereira, J. and
555 Papale, D.: On the differential advantages of evergreenness and deciduousness in mediterranean
556 oak woodlands: A flux perspective, *Ecol. Appl.*, 20(6), 1583–1597, doi:10.1890/08-2047.1, 2010.
557 Barbour, M. M.: Stable oxygen isotope composition of plant tissue: a review, *Funct. Plant Biol.*,
558 34, 83–94, doi:10.1071/FP06228, 2007.

559 | Barbour, M. M., Cernusak, L. A. and Farquhar, G. D.: Factors affecting the oxygen isotope ratio

Unknown

Code de champ modifié

Unknown

Code de champ modifié

Aliénor Lavergne 29/9/y 13:10

Supprimé: Farquhar

561 of plant organic material, in *Stable isotopes and biosphere-atmosphere interactions: Processes*
562 *and Biological Controls*, edited by L. B. Flanagan, J. R. Ehleringer, and D. E. Pataki, pp. 9–28,
563 Elsevier, Amsterdam., 2005.

564 Boucher, E., Guiot, J., Hatté, C., Daux, V., Danis, P. A. and Dussouillez, P.: An inverse modeling
565 approach for tree-ring-based climate reconstructions under changing atmospheric CO₂
566 concentrations, *Biogeosciences*, 11(12), 3245–3258, 2014.

567 Brienen, R. J. W., Helle, G., Pons, T. L., Guyot, J.-L. and Gloor, M.: Oxygen isotopes in tree
568 rings are a good proxy for Amazon precipitation and El Niño-Southern Oscillation variability,
569 *Proc. Natl. Acad. Sci.*, 109(42), 16957–16962, doi:10.1073/pnas.1205977109, 2012.

570 Buhay, W. M., Edwards, T. W. D. and Aravena, R.: Evaluating kinetic fractionation factors used
571 for reconstructions from oxygen and hydrogen isotope ratios in plant water and cellulose,
572 *Geochemistry, Geophys. Geosystems*, 60(12), 2209–2218, 1996.

573 Cernusak, L. A. and English, N. B.: Beyond tree-ring widths: stable isotopes sharpen the focus on
574 climate responses of temperate forest trees, *Tree Physiol.*, 35(1), 1–3,
575 doi:10.1093/treephys/tpu115, 2015.

576 Compo, G. P., Whitaker, J. S., Sardeshmukh, P. D., Matsui, N., Allan, R. J., Yin, X., Gleason, B.
577 E., Vose, R. S., Rutledge, G., Bessemoulin, P., BroNnimann, S., Brunet, M., Crouthamel, R. I.,
578 Grant, A. N., Groisman, P. Y., Jones, P. D., Kruk, M. C., Kruger, A. C., Marshall, G. J., Maugeri,
579 M., Mok, H. Y., Nordli, O., Ross, T. F., Trigo, R. M., Wang, X. L., Woodruff, S. D. and Worley,
580 S. J.: The *twentieth century reanalysis project*, *Q. J. R. Meteorol. Soc.*, 137(654), 1–28,
581 doi:10.1002/qj.776, 2011.

582 Craig, H. and Gordon, L. I.: Deuterium and oxygen 18 variations in the ocean and the marine
583 atmosphere, *Spoletto*, 1965.

584 Danis, P. A., Hatté, C., Misson, L. and Guiot, J.: MAIDENiso: a multiproxy biophysical model of
585 tree-ring width and oxygen and carbon isotopes, *Can. J. For. Res.*, 42(9), 1697–1713,
586 doi:10.1139/x2012-089, 2012.

587 Danis, P. A., Masson-Delmotte, V., Stievenard, M., Guillemin, M. T., Daux, V., Naveau, P. and
588 von Grafenstein, U.: Reconstruction of past precipitation δ¹⁸O using tree-ring cellulose δ¹⁸O and
589 δ¹³C: A calibration study near Lac d'Annecy, France, *Earth Planet. Sci. Lett.*, 243(3–4), 439–448,
590 doi:10.1016/j.epsl.2006.01.023, 2006.

591 Dansgaard, W.: Stable isotopes in precipitation, *Tellus A*, 16(4), 436–468,

Aliénor Lavergne 29/9/y 16:55
Supprimé: Isotopes

Aliénor Lavergne 29/9/y 16:55
Supprimé: Biosphere

Aliénor Lavergne 29/9/y 16:55
Supprimé: Atmosphere

Aliénor Lavergne 29/9/y 15:53
Mis en forme ... [2]

Aliénor Lavergne 29/9/y 16:55
Supprimé: Interactions

Aliénor Lavergne 29/9/y 12:46
Supprimé: a

Aliénor Lavergne 29/9/y 15:53
Mis en forme ... [3]

Aliénor Lavergne 29/9/y 15:53
Mis en forme ... [4]

Aliénor Lavergne 29/9/y 12:52
Supprimé: n

Aliénor Lavergne 29/9/y 12:54
Supprimé: a

Aliénor Lavergne 29/9/y 16:56
Supprimé: Twentieth

Aliénor Lavergne 29/9/y 15:53
Mis en forme ... [5]

Aliénor Lavergne 29/9/y 16:56
Supprimé: Century

Aliénor Lavergne 29/9/y 15:53
Mis en forme ... [6]

Aliénor Lavergne 29/9/y 16:56
Supprimé: Reanalysis

Aliénor Lavergne 29/9/y 15:53
Mis en forme ... [7]

Aliénor Lavergne 29/9/y 16:56
Supprimé: Project

Aliénor Lavergne 29/9/y 15:53
Mis en forme ... [8]

Aliénor Lavergne 29/9/y 12:46
Supprimé: . [online] Available from: ... [9]

Aliénor Lavergne 29/9/y 12:56
Supprimé: -

Aliénor Lavergne 29/9/y 15:53
Mis en forme ... [10]

Aliénor Lavergne 29/9/y 15:53
Mis en forme ... [11]

Aliénor Lavergne 29/9/y 15:53
Mis en forme ... [12]

Aliénor Lavergne 29/9/y 15:53
Mis en forme ... [13]

Aliénor Lavergne 29/9/y 15:53
Mis en forme ... [14]

Aliénor Lavergne 29/9/y 15:53
Mis en forme ... [15]

609 doi:10.3402/tellusa.v16i4.8993, 1964.

610 DeNiro, M. J. and Epstein, S.: Relationship between the oxygen isotope ratios of terrestrial plant
611 cellulose, carbon dioxide, and water, *Science*, 204, 51-53, 1979.

612 DeNiro, M. J. and Epstein, S.: Isotopic composition of cellulose from aquatic organisms,
613 *Geochim. Cosmochim. Acta*, 45(10), 1885–1894, doi:10.1016/0016-7037(81)90018-1, 1981.

614 Donoso, C.: Tipos forestales de los bosques nativos de Chile., Documento de Trabajo Nu. 38.
615 Investigación y Desarrollo Forestal (CONAF, PNUD-FAO). FAO Chile., 1981.

616 Farquhar, G. D., Barbour, M. M. and Henry, B. K.: Interpretation of oxygen isotope composition
617 of leaf material, in *Stable isotopes: integration of biological, ecological and geochemical*
618 *processes*, pp. 27–61, BIOS Scientific Publishers: Oxford., 1998.

619 Farquhar, G. D., Hubick, H. T., Condon, A. G. and Richards, R. A.: Carbon isotope fractionation
620 and plant water-use efficiency, in *Stable isotopes in ecological research*, pp. 21–40., 1989.

621 Gea-Izquierdo, G., Guibal, F., Joffre, R., Ourcival, J. M., Simioni, G. and Guiot, J.: Modelling
622 the climatic drivers determining photosynthesis and carbon allocation in evergreen Mediterranean
623 forests using multiproxy long time series, *Biogeosciences*, 12(12), 3695–3712, doi:10.5194/bg-
624 12-3695-2015, 2015.

625 Gennaretti, F., Arseneault, D., Nicault, A., Perreault, L. and Bégin, Y.: Volcano-induced regime
626 shifts in millennial tree-ring chronologies from northeastern North America., *Proc. Natl. Acad.*
627 *Sci. U. S. A.*, 111(28), 10077-10082, doi:10.1073/pnas.1324220111, 2014.

628 Gennaretti, F., Gea-Izquierdo, G., Boucher, E., Berninger, F., Arseneault, D. and Guiot, J.:
629 Ecophysiological modeling of the climate imprint on photosynthesis and carbon allocation to the
630 tree stem in the North American boreal forest, *Biogeosciences Discuss.*, *in review*,
631 doi:10.5194/bg-2017-51, 2017a.

632 Gennaretti, F., Huard, D., Naulier, M., Savard, M., Bégin, C., Arseneault, D. and Guiot, J.:
633 Bayesian multiproxy temperature reconstruction with black spruce ring widths and stable
634 isotopes from the northern Quebec taiga, *Clim. Dyn.*, 1–13, doi:10.1007/s00382-017-3565-5,
635 2017b.

636 Gessler, A., Ferrio, J. P., Hommel, R., Treydte, K., Werner, R. A. and Monson, R. K.: Stable
637 isotopes in tree rings: towards a mechanistic understanding of isotope fractionation and mixing
638 processes from the leaves to the wood., *Tree Physiol.*, 0, 1–23, 2014.

639 Guiot, J., Boucher, E. and Gea-Izquierdo, G.: Process models and model-data fusion in

Aliénor Lavergne 29/9/y 12:57

Supprimé: (80-.)

Aliénor Lavergne 29/9/y 12:58

Supprimé: (April)

Aliénor Lavergne 29/9/y 12:58

Supprimé: 6–8

Aliénor Lavergne 29/9/y 16:56

Supprimé: Isotopes

Aliénor Lavergne 29/9/y 16:56

Supprimé: Ecological

Aliénor Lavergne 29/9/y 15:53

Mis en forme: Anglais (G.B.)

Aliénor Lavergne 29/9/y 16:56

Supprimé: Research

Aliénor Lavergne 29/9/y 13:01

Supprimé: (22)

Aliénor Lavergne 29/9/y 13:01

Supprimé:)

Aliénor Lavergne 29/9/y 13:18

Supprimé: (February), 1–26,

Aliénor Lavergne 29/9/y 13:01

Supprimé: (123456789),

Aliénor Lavergne 29/9/y 12:59

Supprimé: [online] Available from:
http://www.ncbi.nlm.nih.gov/pubmed/24907466
(Accessed 11 July 2014)

653 dendroecology, *Front. Ecol. Evol.*, 2, 52, doi:10.3389/fevo.2014.00052, 2014.

654 Hartl-Meier, C., Zang, C., Büntgen, U. L. F., Esper, J. A. N., Rothe, A., Göttelein, A., Dirnböck,
655 T. and Treydte, K.: Uniform climate sensitivity in tree-ring stable isotopes across species and
656 sites in a mid-latitude temperate forest., *Tree Physiol.*, 2003(1), 4–15,
657 doi:10.1093/treephys/tpu096, 2014.

658 Helliker, B. R. and Richter, S. L.: Subtropical to boreal convergence of tree-leaf temperatures,
659 *Nature*, 454(7203), 511–514, doi:10.1038/nature07031, 2008.

660 Horita, J. and Wesolowski, D. J.: Liquid-vapor fractionation of oxygen and hydrogen isotopes of
661 water from the freezing to the critical temperature, *Geochim. Cosmochim. Acta*, 58(16), 3425–
662 3437, doi:10.1016/0016-7037(94)90096-5, 1994.

663 Hourdin, F., Grandpeix, J. Y., Rio, C., Bony, S., Jam, A., Cheruy, F., Rochetin, N., Fairhead, L.,
664 Idelkadi, A., Musat, I., Dufresne, J. L., Lahellec, A., Lefebvre, M. P. and Roehrig, R.: LMDZ5B:
665 The atmospheric component of the IPSL climate model with revisited parameterizations for
666 clouds and convection, *Clim. Dyn.*, 40(9–10), 2193–2222, doi:10.1007/s00382-012-1343-y,
667 2013.

668 Hutchinson, M. F., McKenney, D. W., Lawrence, K., Pedlar, J. H., Hopkinson, R. F., Milewska,
669 E. and Papadopol, P.: Development and testing of Canada-wide interpolated spatial models of
670 daily minimum-maximum temperature and precipitation for 1961-2003, *J. Appl. Meteorol.*
671 *Climatol.*, 48(4), 725–741, doi:10.1175/2008JAMC1979.1, 2009.

672 Insel, N., Poulsen, C. J., Sturm, C. and Ehlers, T. A.: Climate controls on Andean precipitation
673 $\delta^{18}\text{O}$ interannual variability, *J. Geophys. Res. Atmos.*, 118(17), 9721–9742,
674 doi:10.1002/jgrd.50619, 2013.

675 Kahmen, A., Sachse, D., Arndt, S. K., Tu, K. P., Farrington, H., Vitousek, P. M. and Dawson, T.
676 E.: Cellulose $\delta^{18}\text{O}$ is an index of leaf-to-air vapor pressure difference (VPD) in tropical plants.,
677 *Proc. Natl. Acad. Sci. U. S. A.*, 108(5), 1981–1986, doi:10.1073/pnas.1018906108, 2011.

678 Keeling, C. D., Bacastow, R. B., Bainbridge, A. E., Ekdahl Jr., C. A., Guenther, P. R.,
679 Waterman, L. S. and Chin, J. F. S.: Atmospheric carbon dioxide variations at Mauna Loa
680 Observatory, Hawaii, *Tellus A*, 28, 538–551, doi:10.3402/tellusa.v28i6.11322, 1976.

681 Labuhn, I., Daux, V., Girardclos, O., Stievenard, M., Pierre, M. and Masson-Delmotte, V.:
682 French summer droughts since 1326 AD: a reconstruction based on tree ring cellulose $\delta^{18}\text{O}$,
683 *Clim. Past*, 11(6), 5113–5155, doi:10.5194/cpd-11-5113-2015, 2016.

Aliénor Lavergne 29/9/y 12:59

Supprimé: (August)

Aliénor Lavergne 29/9/y 13:01

Supprimé: (delta)

Aliénor Lavergne 29/9/y 13:02

Supprimé: .

687 Lavergne, A., Daux, V., Villalba, R. and Barichivich, J.: Temporal changes in climatic limitation
688 of tree-growth at upper treeline forests: Contrasted responses along the west-to-east humidity
689 gradient in Northern Patagonia, *Dendrochronologia*, 36, 49–59, 2015.

690 Lavergne, A., Daux, V., Villalba, R., Pierre, M., Stievenard, M. and Srur, A. M.: Improvement of
691 isotope-based climate reconstructions in Patagonia through a better understanding of climate
692 influences on isotopic fractionation in tree rings, *Earth Planet. Sci. Lett.*, 459, 372–380,
693 doi:10.1016/j.epsl.2016.11.045, 2017.

694 Lavergne, A., Daux, V., Villalba, R., Pierre, M., Stievenard, M., Srur, A. M. and Vimeux, F.: Are
695 the $\delta^{18}\text{O}$ of *F. cupressoides* and *N. pumilio* promising proxies for climate reconstructions in
696 northern Patagonia?, *J. Geophys. Res. - Biogeosciences*, 121(3), 767–776,
697 doi:10.1002/2015JG003260, 2016.

698 López Bernal, P., Defossé, G. E., Quinteros, C. P. and Bava, J. O.: Sustainable management of
699 lenga (*Nothofagus pumilio*) forests through group selection system, in *Sustainable forest*
700 management - current research, edited by D. J. J. D. (Ed.), pp. 45–66, 2012.

701 Lorrey, A. M., Brookman, T. H., Evans, M. N., Fauchereau, N.C., Barbour, M., Macinnis-Ng, C.
702 Criscitiello, A., Eischeid, G., Fowler, A. M., Horton, T. W. and Schrag, D. P.: Stable oxygen
703 isotope signatures of early season wood in New Zealand kauri (*Agathis australis*) tree rings:
704 Prospects for palaeoclimate reconstruction., *Dendrochronologia*, 40, 50–63, doi:
705 10.1016/j.dendro.2016.03.012, 2016.

706 Magnin, A., Puntieri, J. and Villalba, R.: Interannual variations in primary and secondary growth
707 of *Nothofagus pumilio* and their relationships with climate, *Trees*, 28(5), 1463–1471, 2014.

708 Misson, L.: MAIDEN: a model for analyzing ecosystem processes in dendroecology, *Can. J. For.*
709 *Res.*, 34, 874–887, 2004.

710 Naulier, M., Savard, M. M., Bégin, C., Gennaretti, F., Arseneault, D., Marion, J., Nicault, A. and
711 Bégin, Y.: A millennial summer temperature reconstruction for northeastern Canada using
712 oxygen isotopes in subfossil trees, *Clim. Past*, 11(9), 1153–1164, doi:10.5194/cp-11-1153-2015,
713 2015.

714 Naulier, M., Savard, M. M., Bégin, C., Marion, J., Arseneault, D. and Bégin, Y.: Carbon and
715 oxygen isotopes of lakeshore black spruce trees in northeastern Canada as proxies for climatic
716 reconstruction, *Chem. Geol.*, 374–375, 37–43, doi:10.1016/j.chemgeo.2014.02.031, 2014.

717 Noone, D. and Simmonds, I.: Associations between $\delta^{18}\text{O}$ of water and climate parameters in a

Aliénor Lavergne 29/9/y 15:53
Mis en forme ... [16]

Aliénor Lavergne 29/9/y 16:57
Supprimé: Management

Aliénor Lavergne 29/9/y 15:53
Mis en forme ... [17]

Aliénor Lavergne 29/9/y 16:57
Supprimé: Lenga

Aliénor Lavergne 29/9/y 16:57
Supprimé: Group

Aliénor Lavergne 29/9/y 16:57
Supprimé: Forest

Aliénor Lavergne 29/9/y 15:53
Mis en forme ... [18]

Aliénor Lavergne 29/9/y 16:57
Supprimé: Forests

Aliénor Lavergne 29/9/y 16:57
Supprimé: Through

Aliénor Lavergne 29/9/y 16:57
Supprimé: Selection

Aliénor Lavergne 29/9/y 16:57
Supprimé: System

Aliénor Lavergne 29/9/y 15:53
Mis en forme ... [19]

Aliénor Lavergne 29/9/y 15:53
Mis en forme ... [20]

Aliénor Lavergne 29/9/y 15:53
Mis en forme ... [21]

Aliénor Lavergne 29/9/y 15:53
Mis en forme ... [22]

Aliénor Lavergne 29/9/y 15:53
Mis en forme ... [23]

Aliénor Lavergne 29/9/y 15:53
Mis en forme ... [24]

Aliénor Lavergne 29/9/y 16:57
Supprimé: Management

Aliénor Lavergne 29/9/y 15:53
Mis en forme ... [25]

Aliénor Lavergne 29/9/y 16:57
Supprimé: Current

Aliénor Lavergne 29/9/y 15:53
Mis en forme ... [26]

Aliénor Lavergne 29/9/y 16:57
Supprimé: Research

Aliénor Lavergne 29/9/y 15:53
Mis en forme ... [27]

Aliénor Lavergne 29/9/y 13:03
Supprimé: , InTech. [online] Available fr ... [28]

Aliénor Lavergne 29/9/y 13:04
Supprimé: https://doi.org/

Aliénor Lavergne 29/9/y 16:58
Supprimé: (February)

Aliénor Lavergne 29/9/y 15:53
Mis en forme ... [29]

755 simulation of atmospheric circulation for 1979–95, *J. Clim.*, 15, 3150–3169, 2002.

756 Ogée, J., Barbour, M. M., Wingate, L., Bert, D., Bosc, A., Stievenard, M., Lambrot, C., Pierre,
757 M., Bariac, T., Loustau, D. and Dewar, R. C.: A single-substrate model to interpret intra-annual
758 stable isotope signals in tree-ring cellulose, *Plant, Cell Environ.*, 32(8), 1071–1090,
759 doi:10.1111/j.1365-3040.2009.01989.x, 2009.

760 Ogée, J., Brunet, Y., Loustau, D., Berbigier, P. and Delzon, S.: MuSICA, a CO₂, water and
761 energy multilayer, multileaf pine forest model: Evaluation from hourly to yearly time scales and
762 sensitivity analysis, *Glob. Chang. Biol.*, 9(5), 697–717, doi:10.1046/j.1365-2486.2003.00628.x,
763 2003.

764 Rinne, K. T., Loader, N. J., Switsur, V. R. and Waterhouse, J. S.: 400-year May-August
765 precipitation reconstruction for Southern England using oxygen isotopes in tree rings, *Quat. Sci.*
766 *Rev.*, 60, 13–25, doi:10.1016/j.quascirev.2012.10.048, 2013.

767 Risi, C., Bony, S., Vimeux, F. and Jouzel, J.: Water-stable isotopes in the LMDZ4 general
768 circulation model: Model evaluation for present-day and past climates and applications to
769 climatic interpretations of tropical isotopic records, *J. Geophys. Res. Atmos.*, 115(12), 1–27,
770 doi:10.1029/2009JD013255, 2010.

771 Roden, J. S., Lin, G. and Ehleringer, J. R.: A mechanistic model for interpretation of hydrogen
772 and oxygen isotope ratios in tree-ring cellulose, *Geochim. Cosmochim. Acta*, 64(1), 21–35,
773 doi:10.1016/S0016-7037(99)00195-7, 2000.

774 Rozanski, K., Araguás-Araguás, L.: Spatial and temporal variability of stable isotope
775 composition of precipitation over the South American continent, *Bull. l'Institut Fr. d'études*
776 *Andin.*, 24(3), 379–390, 1995.

777 Rozanski, K., Araguás-Araguás, L. and Gonfiantini, R.: Isotopic patterns in modern global
778 precipitation, in *Climate change in continental isotopic records*, edited by P. K. Swart, K. C.
779 Lohmann, J. McKenzie, and S. Savin, American Geophysical Union., 1993.

780 Running, S. W., Nemani, R. R. and Hungerford, R. D.: Extrapolation of synoptic meteorological
781 data in mountainous terrain and its use for simulating forest evapotranspiration and
782 photosynthesis, *Can. J. For. Res.*, 17, 472–483, doi:10.1139/x87-081, 1987.

783 Rusch, V. E.: Altitudinal variation in the phenology of *Nothofagus pumilio* in Argentina, *Rev.*
784 *Chil. Hist. Nat.*, 66(2), 131–141, 1993.

785 Saurer, M., Aellen, K. and Siegwolf, R. T. W.: Correlating $\delta^{13}\text{C}$ and $\delta^{18}\text{O}$ in cellulose of trees,

Aliénor Lavergne 29/9/y 13:34

Supprimé: and Araguás, L. A.

Aliénor Lavergne 29/9/y 16:55

Supprimé: Patterns

Aliénor Lavergne 29/9/y 16:55

Supprimé: Modern

Aliénor Lavergne 29/9/y 16:55

Supprimé: Global

Aliénor Lavergne 29/9/y 16:55

Supprimé: Precipitation

Aliénor Lavergne 29/9/y 16:55

Supprimé: Change

Aliénor Lavergne 29/9/y 16:55

Supprimé: Continental

Aliénor Lavergne 29/9/y 16:55

Supprimé: Isotopic

Aliénor Lavergne 29/9/y 16:55

Supprimé: Records

Aliénor Lavergne 29/9/y 13:05

Supprimé: ^d

Aliénor Lavergne 29/9/y 13:05

Supprimé: ^d

797 | Plant, Cell Environ., 20, 1543–1550, 1997.

798 | Saurer, M., Cherubini, P., Reynolds-Henne, C. E., Treydte, K. S., Anderson, W. T. and Siegwolf,
799 | R. T. W.: An investigation of the common signal in tree ring stable isotope chronologies at
800 | temperate sites, J. Geophys. Res. Biogeosciences, 113(4), doi:10.1029/2008JG000689, 2008.

801 | Schlatter, J.: Requerimientos de sitio para la lenga, Nothofagus pumilio (Poepp. et Endl.) Krasser,
802 | Bosque, 15, 3–10, 1994.

803 | Shi, C., Daux, V., Zhang, Q. B., Risi, C., Hou, S. G., Stievenard, M., Pierre, M., Li, Z. and
804 | Masson-Delmotte, V.: Reconstruction of southeast Tibetan Plateau summer climate using tree
805 | ring $\delta^{18}\text{O}$: Moisture variability over the past two centuries, Clim. Past, 8(1), 205–213,
806 | doi:10.5194/cp-8-205-2012, 2012.

807 | Smith, R. B. and Evans, J. P.: Orographic precipitation and water vapor fractionation over the
808 | Southern Andes, J. Hydrometeorol., 8(1), 3–19, doi:10.1175/JHM555.1, 2007.

809 | Stern, L. A. and Blisniuk, P. M.: Stable isotope composition of precipitation across the southern
810 | Patagonian Andes, J. Geophys. Res. Atmos., 107(23), doi:10.1029/2002JD002509p, 2002.

811 | Sternberg, L. D. S. L.: Oxygen and hydrogen isotope ratios in plant cellulose: Mechanisms and
812 | applications, in Stable isotopes in ecological research, edited by J. R. E. and K. A. N. P. W.
813 | Rundel, pp. 124–141., 1989.

814 | Sternberg, L. D. S. L. and Ellsworth, P. F. V.: Divergent biochemical fractionation, not
815 | convergent temperature, explains cellulose oxygen isotope enrichment across latitudes, PLoS
816 | One, 6(11), e28040, doi:10.1371/journal.pone.0028040, 2011.

817 | Sturm, C., Vimeux, F. and Krinner, G.: Intraseasonal variability in South America recorded in
818 | stable water isotopes, J. Geophys. Res. Atmos., 112(20), doi:10.1029/2006JD008298, 2007.

819 | Sturm, K., Hoffmann, G., Langmann, B. and Stichler, W.: Simulation of $\delta^{18}\text{O}$ in precipitation by
820 | the regional circulation model REMOiso, Hydrol. Process., 19(17), 3425–3444,
821 | doi:10.1002/hyp.5979, 2005.

822 | Treydte, K., Boda, S., Graf Pannatier, E., Fonti, P., Frank, D., Ullrich, B., Saurer, M., Siegwolf,
823 | R. T. W., Battipaglia, G., Werner, W. and Gessler, A.: Seasonal transfer of oxygen isotopes from
824 | precipitation and soil to the tree ring: Source water versus needle water enrichment, New Phytol.,
825 | 202(3), 772–783, doi:10.1111/nph.12741, 2014.

826 | Viereck, L. A. and Johnston, W. F.: Picea mariana (Mill.) B. S. P., in Silvics of North America:
827 | 1. Conifers; 2. Hardwoods., edited by R. M. Burns and B. H. Honkala, pp. 443–464, US.

Aliénor Lavergne 29/9/y 13:05

Supprimé: doi:S,

Aliénor Lavergne 29/9/y 16:59

Supprimé: Precipitation

Aliénor Lavergne 29/9/y 16:59

Supprimé: Water

Aliénor Lavergne 29/9/y 16:59

Supprimé: Vapor

Aliénor Lavergne 29/9/y 15:53

Mis en forme: Anglais (G.B.)

Aliénor Lavergne 29/9/y 16:59

Supprimé: Fractionation

Aliénor Lavergne 29/9/y 13:05

Supprimé: a

Aliénor Lavergne 29/9/y 16:59

Supprimé: Isotopes

Aliénor Lavergne 29/9/y 16:59

Supprimé: Ecological

Aliénor Lavergne 29/9/y 16:59

Supprimé: Research

Aliénor Lavergne 29/9/y 16:59

Supprimé:

838 Department of Agriculture, Forest Service, Washington, DC., 1990.
 839 Wernicke, J., Griebinger, J., Hochreuther, P. and Brauning, A.: Variability of summer humidity
 840 during the past 800 years on the eastern Tibetan Plateau inferred from $\delta^{18}\text{O}$ of tree-ring cellulose.,
 841 Clim. Past, 11, 327–337, doi:10.5194/cp-11-327-2015, 2015.
 842 Wershaw, R. L., Friedman, I. and Heller, S. J.: Hydrogen isotope fractionation in water passing
 843 through trees, in Advances in Organic Geochemistry, edited by F. Hobson and M. Speers, pp. 55–
 844 67, New York, Pergamon., 1966.
 845 Yakir, D. and DeNiro, M. J.: Oxygen and [hydrogen isotope fractionation during cellulose](#)
 846 [metabolism in *Jemna* gibba L.](#), Plant Physiol., 93(1), 325–332, doi:10.1104/pp.93.1.325, 1990.

847 848 Tables and Figures

850 **Table 1** Definition of sensitive parameters. The posterior medians and 90% confidence intervals
 851 are also shown.

Parameter	Definition	Unit	Parameter type (prior range)	Values with 90% posterior confidence intervals
f_0	Dampening factor	NA	Calibrated (0.3 to 0.5)	0.36 [0.31; 0.46] (Arg.) 0.41 [0.32; 0.48] (Q.)
ϵ_0	Biochemical fractionation	‰	Calibrated (24 to 30)	29.99 [29.93; 30] (Arg.) 26.81 [24.74; 28.04] (Q.)
ϵ_k	Kinetic fractionation	‰	Calibrated (10 to 30)	28.86 [18.25; 29.96] (Arg.) 17.20 [11.16; 26.34] (Q.)
a	Temperature dependence of $\delta^{18}\text{O}_p$	NA	Calibrated (0.2 to 0.5 for Arg. and 0 to 0.38 for Q.)	0.50 [0.49; 0.50] (Arg.) 0.31 [0.25; 0.37] (Q.)
b	Precipitation dependence of $\delta^{18}\text{O}_p$	NA	Calibrated (-0.3 to 0 for Arg. and -0.39 to 0 for Q.)	-0.009 [-0.15; 0] (Arg.) -0.22 [-0.35; -0.14] (Q.)
c	Intercept of $\delta^{18}\text{O}_p$	‰	Fixed	-10.0 (Arg.) -11.9 (Q.)

853
854
855
856

- Aliénor Lavergne 29/9/y 17:00
Supprimé: Hydrogen
- Aliénor Lavergne 29/9/y 17:00
Supprimé: Isotope
- Aliénor Lavergne 29/9/y 17:00
Supprimé: Fractionation
- Aliénor Lavergne 29/9/y 17:00
Supprimé: Cellulose
- Aliénor Lavergne 29/9/y 17:00
Supprimé: Metabolism
- Aliénor Lavergne 29/9/y 17:00
Supprimé: Lemna

863 **Table 2** Climate input data for all tested simulations

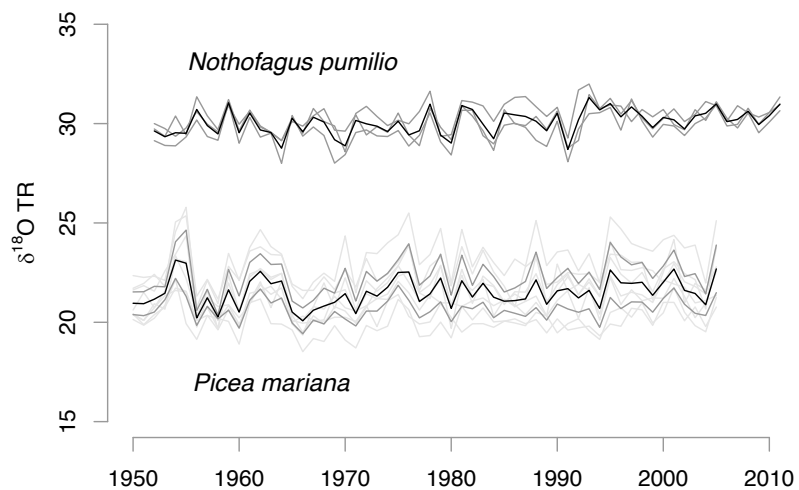
864

	Daily Tmin and Tmax	Daily P	Daily $\delta^{18}\text{O}_p$	CO ₂
Configuration 1	Canadian database/ NOAA-CIRES dataset		Linear regression	Mauna
Configuration 2	Canadian database / NOAA-CIRES dataset		MUGCM data	Loa
Configuration 3	LMDZ-NCEP20 data			station

865

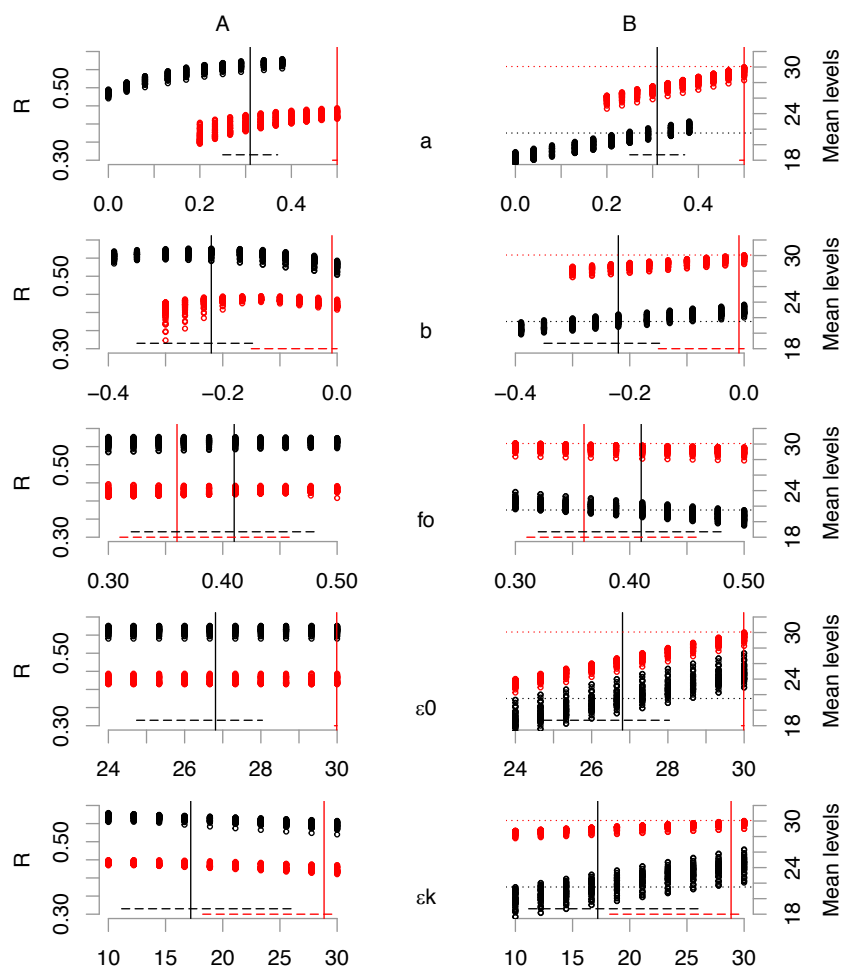
866

867 **Figure 1** Tree-ring $\delta^{18}\text{O}$ time series (%) at the three sites in Argentina (NUB, ALM and CHA in
868 dark grey) and two sites in Quebec (L01 and L20 in dark grey; single trees in light grey). The
869 bold black lines are the averaged values. The mean inter-site correlation coefficients are
870 $r = 0.60$, $p < 0.05$ and $r = 0.80$, $p < 0.01$ in the South and North American sites, respectively.
871

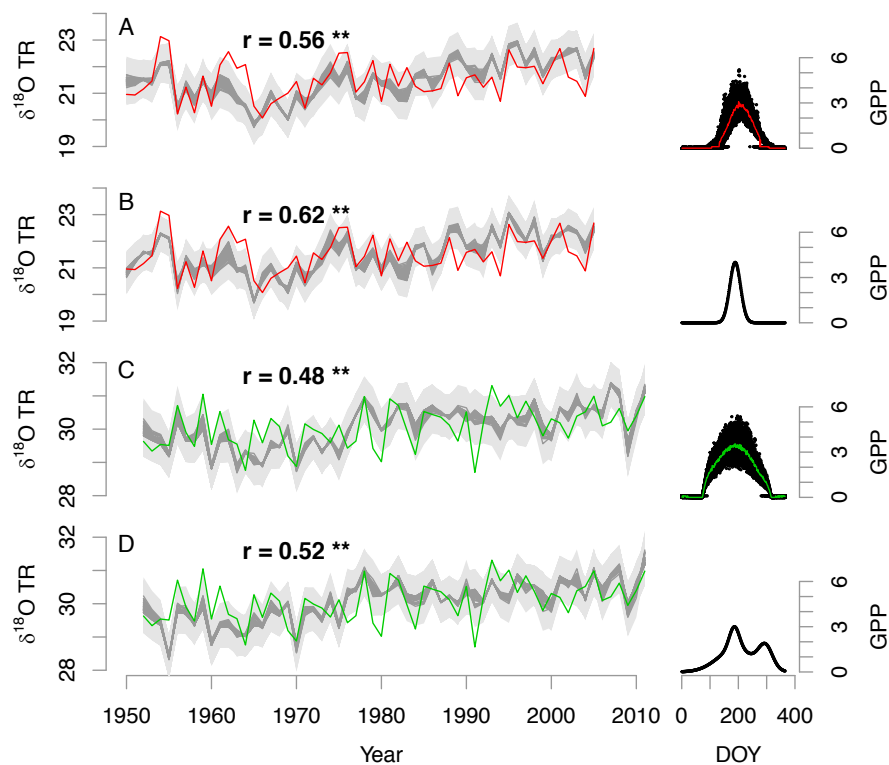


872
873

874 **Figure 2** Dependence of the correlation coefficients between observed and simulated $\delta^{18}\text{O}_{\text{TR}}$
 875 series (panels A), and of the mean simulated $\delta^{18}\text{O}_{\text{TR}}$ levels (‰) (panels B) as a function of the
 876 range of calibrated parameters a , b , f_o , ϵ_0 and ϵ_k for the 50 simulations performed. In black are the
 877 tests with the sites from Quebec and in red the ones with the Argentinean sites. The vertical lines
 878 are the values of a plausible block of parameters retained in the MCMC optimization. The
 879 horizontal dashed lines are their respective 90% confidence interval calculated with 50
 880 simulations (see Table 1). The horizontal dot lines in panel B are the mean values of the observed
 881 $\delta^{18}\text{O}_{\text{TR}}$.

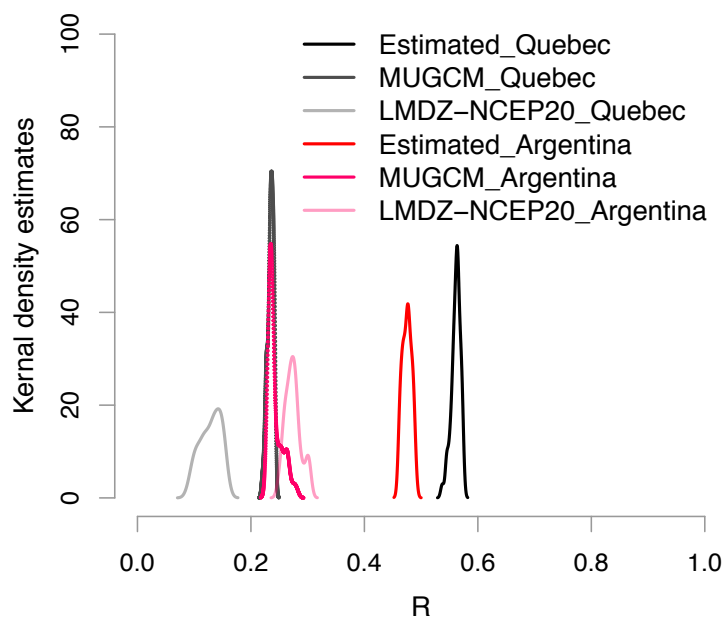


883 **Figure 3** Comparison between observed (red or green) and simulated (grey) $\delta^{18}\text{O}_{\text{TR}}$ chronologies
 884 in Quebec (A and B) and Argentina (C and D), respectively, using GPP (in $\text{gC}\cdot\text{m}^{-2}\cdot\text{day}^{-1}$)
 885 simulated by MAIDENiso (A and C) or synthesized for maximizing correlations (B and D). The
 886 simulations are based on estimated $\delta^{18}\text{O}_{\text{p}}$ series. The 50 different simulations inferred from the
 887 Markov Chain Monte Carlo (MCMC) chains are in dark grey. The ± 1 root mean square error
 888 (RMSE) range is represented in light grey. The mean correlation coefficients are significant at
 889 99% level (**).



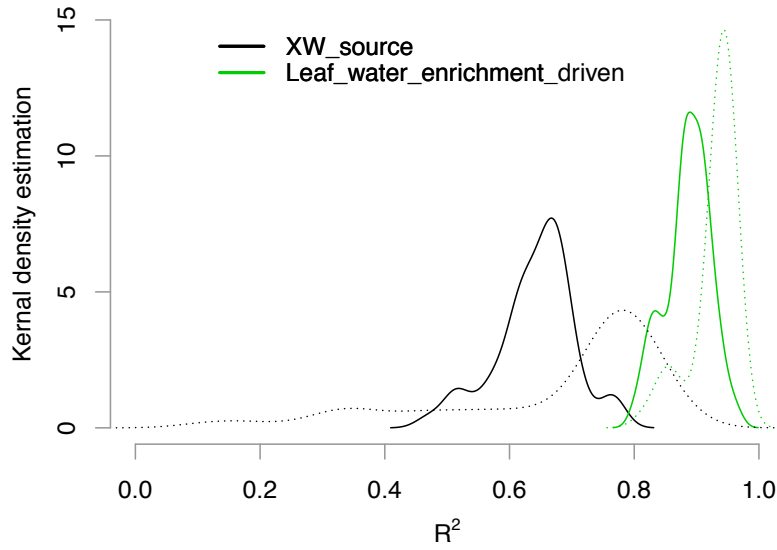
890
 891

892 **Figure 4** Comparison of the densities of probability of the coefficient of correlation (R) between
893 observed and simulated $\delta^{18}\text{O}_{\text{TR}}$ chronologies in Quebec and Argentina when the simulations are
894 based on $\delta^{18}\text{O}_{\text{P}}$ series estimated by the regression model or from the MUGCM and LMDZ-
895 NCEP20 models.
896



897
898

899 **Figure 5** Density distributions of the coefficients of determination (R^2) between the reference
900 | simulations and the: 1) XW_source experiment simulation ($\delta^{18}O_V$ and h_{air} set as constant, black)
901 | and, 2) Leaf_water_enrichment_driven experiment simulation ($\delta^{18}O_{XW}$ set as constant, green) in
902 | Quebec (bold line) and Argentina (dashed line).



903
904
905

Aliénor Lavergne 2/10/y 15:58
Supprimé: _
Aliénor Lavergne 2/10/y 15:58
Supprimé: _
Aliénor Lavergne 2/10/y 15:58
Supprimé: _
Aliénor Lavergne 2/10/y 15:58
Supprimé: _